Fermi-LAT point source population studies and origin of the Fermi-LAT gamma-ray background

Mattia Di Mauro

Stanford University

SLAC NATIONAL ACCELERATOR LABORATORY

On behalf of the Fermi-LAT Collaboration

Trieste, May, 3, 2016

THE ISOTROPIC GAMMA RAY BACKGROUND

IGRB first discovered by **OSO-3** (then by **SAS-2** and **EGRET)**

V. SUMMARY OF RESULTS

1) The OSO-3 γ-ray detector operated as planned for sixteen months in orbit and recorded 621 events caused almost entirely by cosmic γ-rays with energies above the threshold of 50 MeV.

2) The celestial distribution of the recorded γ-rays is highly anisotropic and shows a 10.4 σ concentration along the galactic equator with an extended region of high intensity around the galactic center.

3) The cosmic γ-rays at high galactic latitudes have a softer energy spectrum than those at low latitudes. No difference is discernible between the spectra of γ-rays from the galactic center region and the rest of the equatorial region.

4) The observations can be accounted for in terms of the following three components: (*a*) a general galactic component which is produced throughout the Galaxy at a rate equal to 1.6×10^{-25} s^{-1} per atom of atomic hydrogen for γ-ray photons with energies above 100 MeV; (*b*) an isotropic, and presumably extragalactic, component with a relatively softer spectrum, and an intensity above 100 MeV of 4.9×10^{-5} (cm^2 s sterad)$^{-1}$; (*c*) a galactic center component emanating from a region extending along the galactic equator for about 30° on either side of the center. The

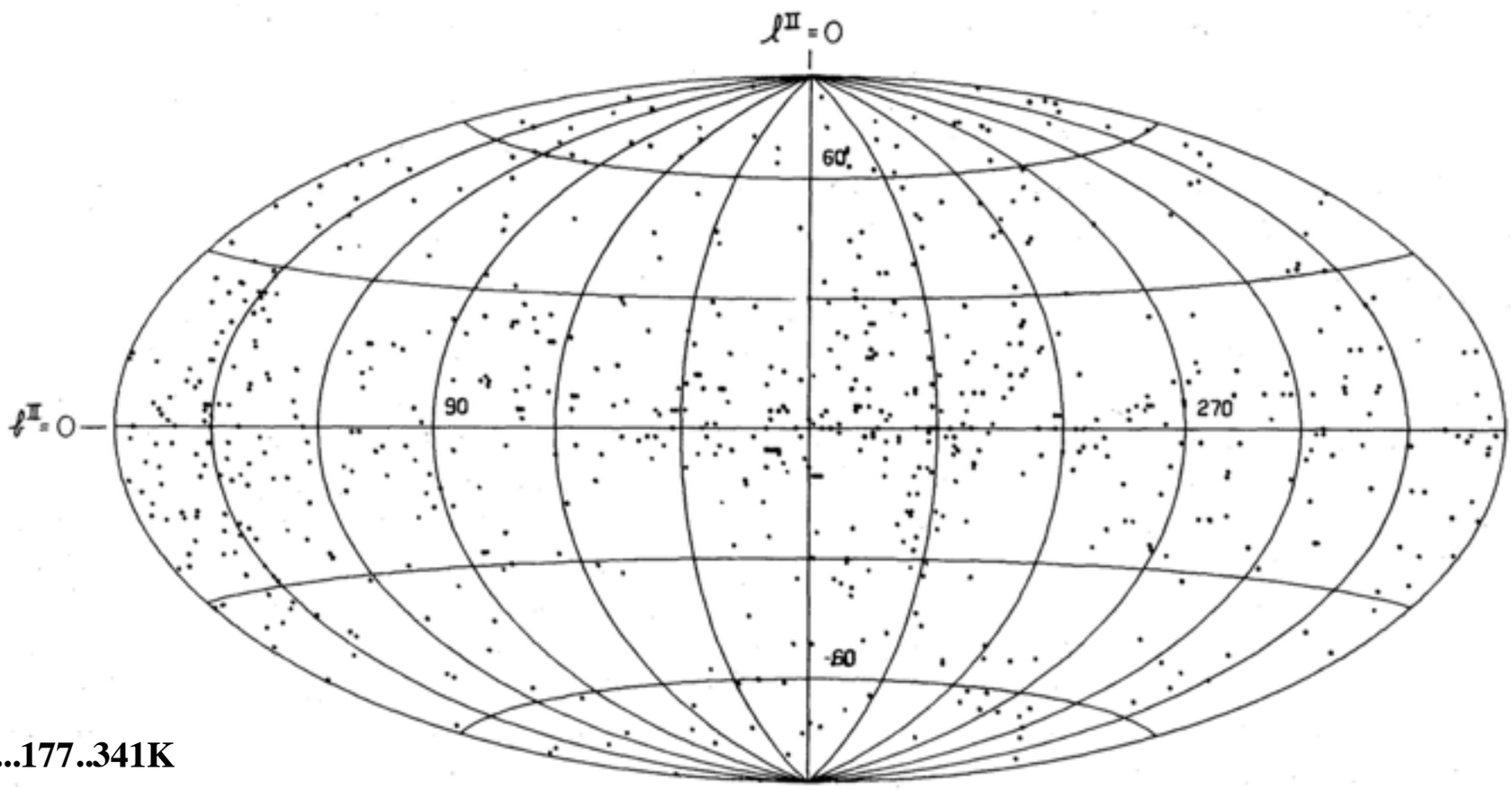

Kraushaar 1972ApJ...177..341K

THE FERMI-LAT GAMMA-RAY SKY

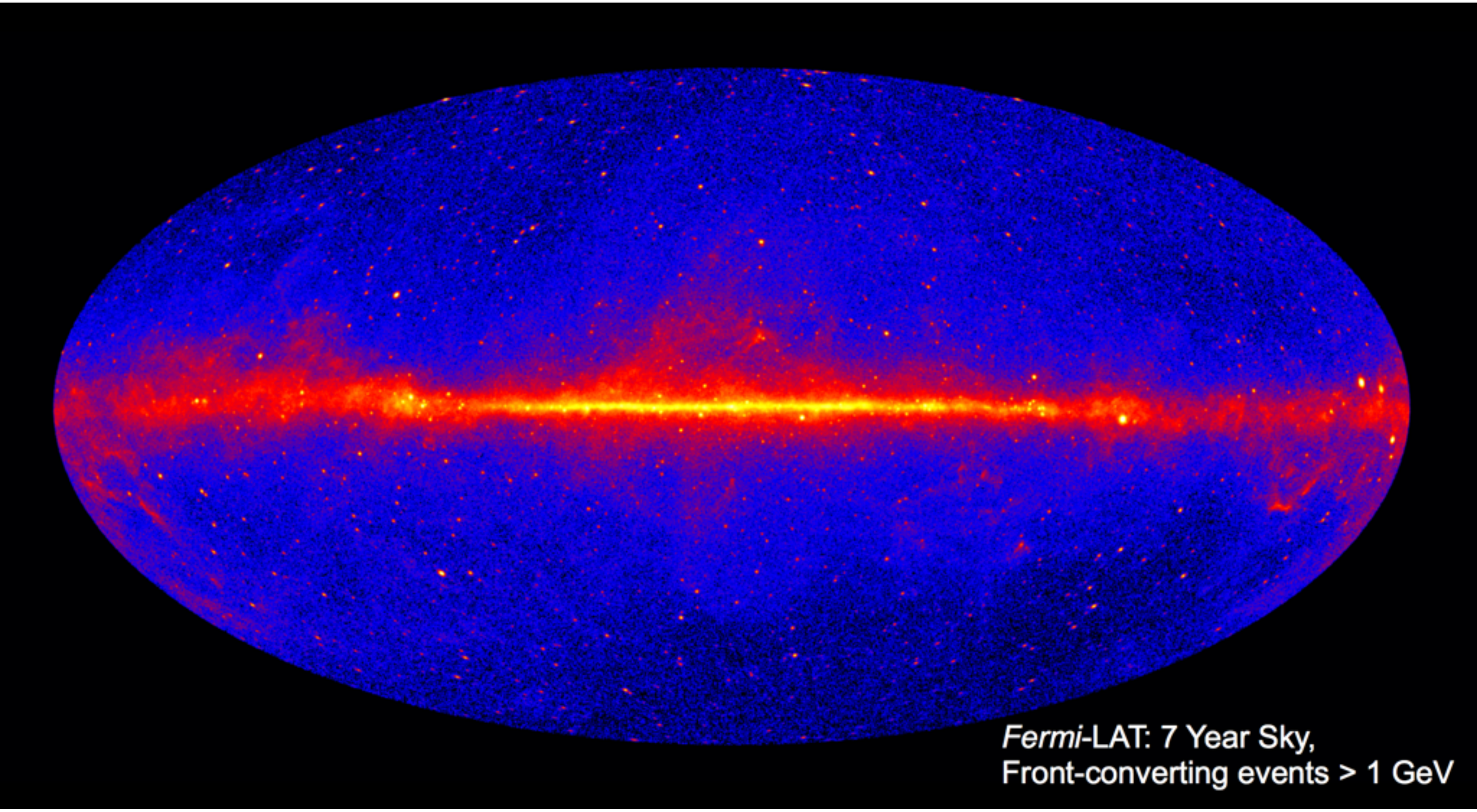

THE FERMI-LAT GAMMA-RAY SKY

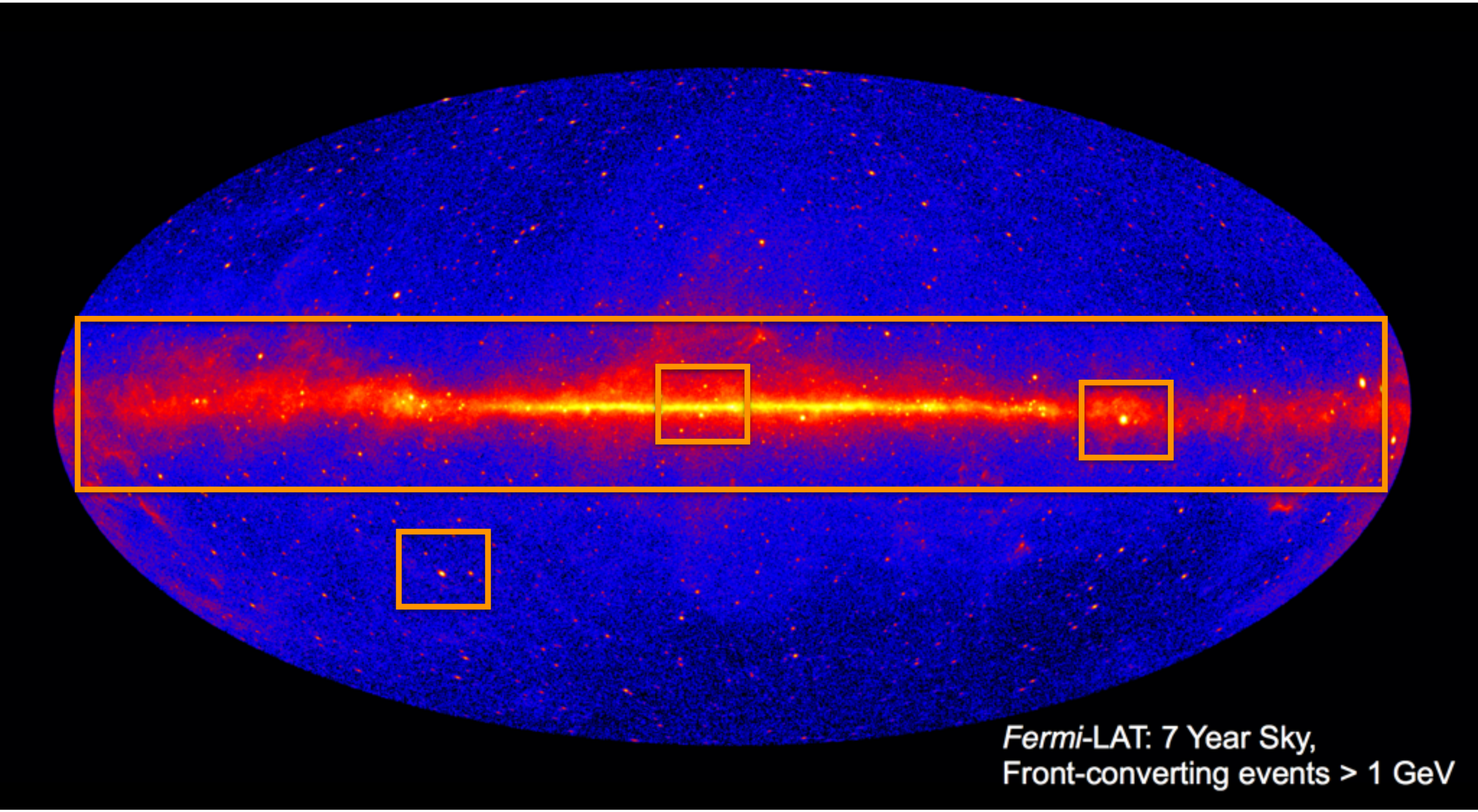

THE FERMI-LAT GAMMA-RAY SKY

- The Fermi Large Area Telescope provides a view of the entire gamma-ray sky from 10 MeV to 2 TeV.

- Galactic diffuse emission (GDE) produced via:

  -decay of π^0 produced in protons/ interstellar gas collisions
  -Bremsstrahlung of relativistic electrons in gas and
  -Inverse-Compton of relativistic electrons with ISRF.

- Solar emission and cosmic ray background

- 2FGL catalog resolved sources.

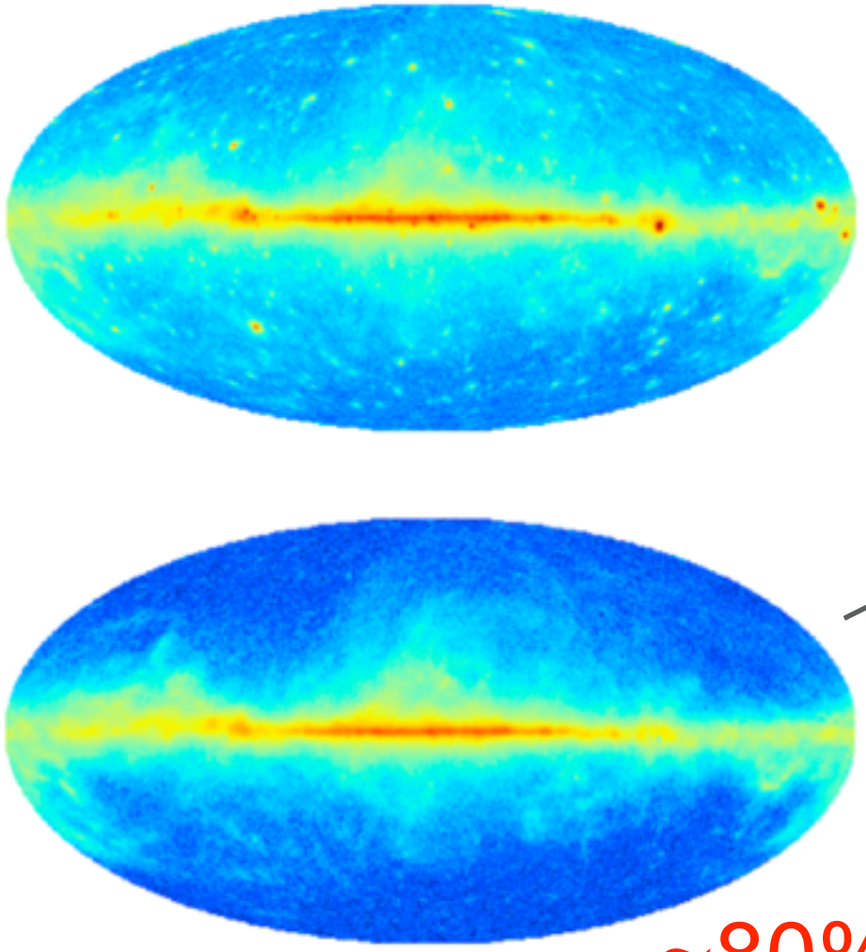

~80%

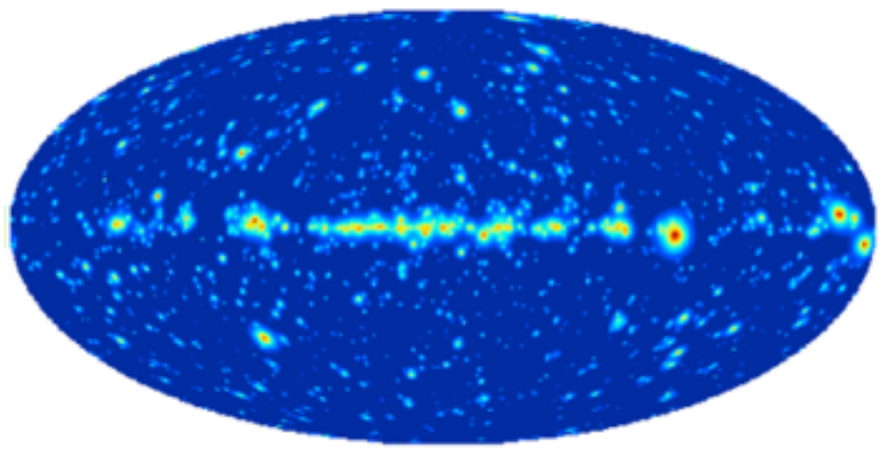

~10%

DATA

–

GDE

–

SUN + CR BACK

=

EGB

–

RESOLVED SOURCES

=

IGRB

Ackermann et al. ApJ 799 (2015) 1, 86
Ackermann et al. Astrophys.J. 750 (2012) 3

FERMI-LAT IGRB AND EGB DATA

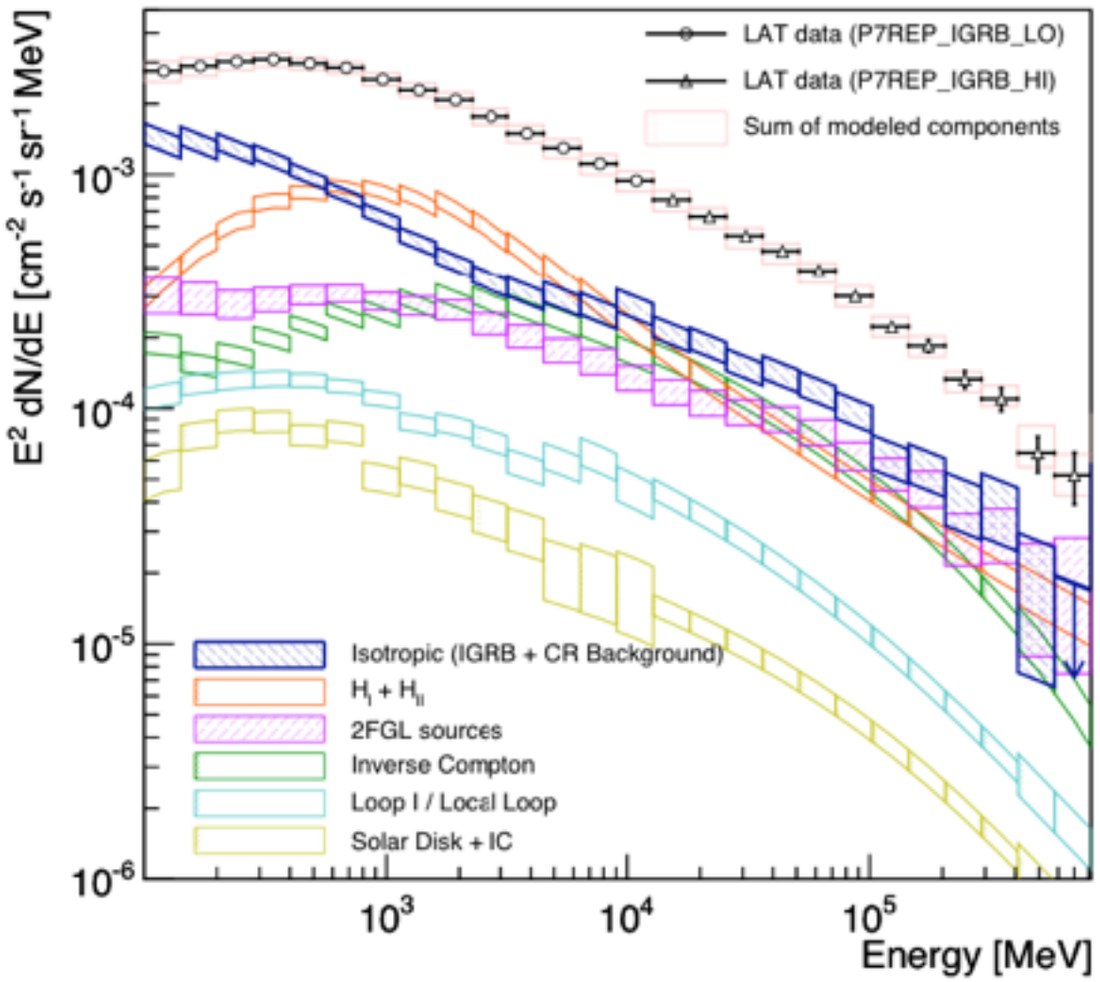

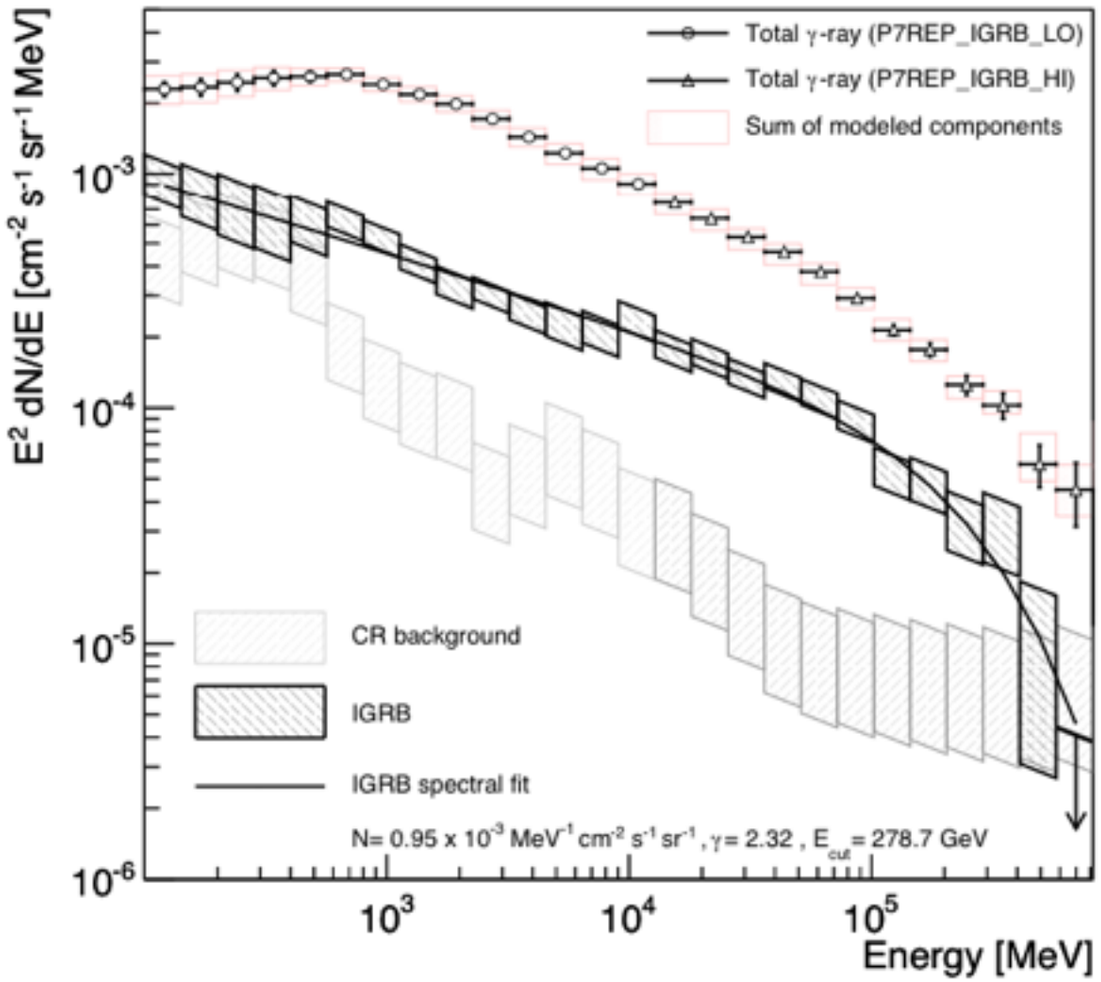

Foreground	Main features and differences with respect to other DGE models
Model A	Sources of CR nuclei and electrons trace pulsar distribution; constant CR diffusion coefficient and re-acceleration strength through Galaxy
Model B	Additional electron-only source population near Galactic center, these electrons are responsible for majority of IC emission; local source of soft CR electrons needed to explain CR electron spectrum at Earth below 20 GV
Model C	Sources of CR nuclei and electrons more centrally peaked than pulsar distribution; CR diffusion coefficient and re-acceleration strength vary with Galactocentric radius and height

Ackermann et al. ApJ 799 (2015) 1, 86

FERMI-LAT IGRB AND EGB DATA

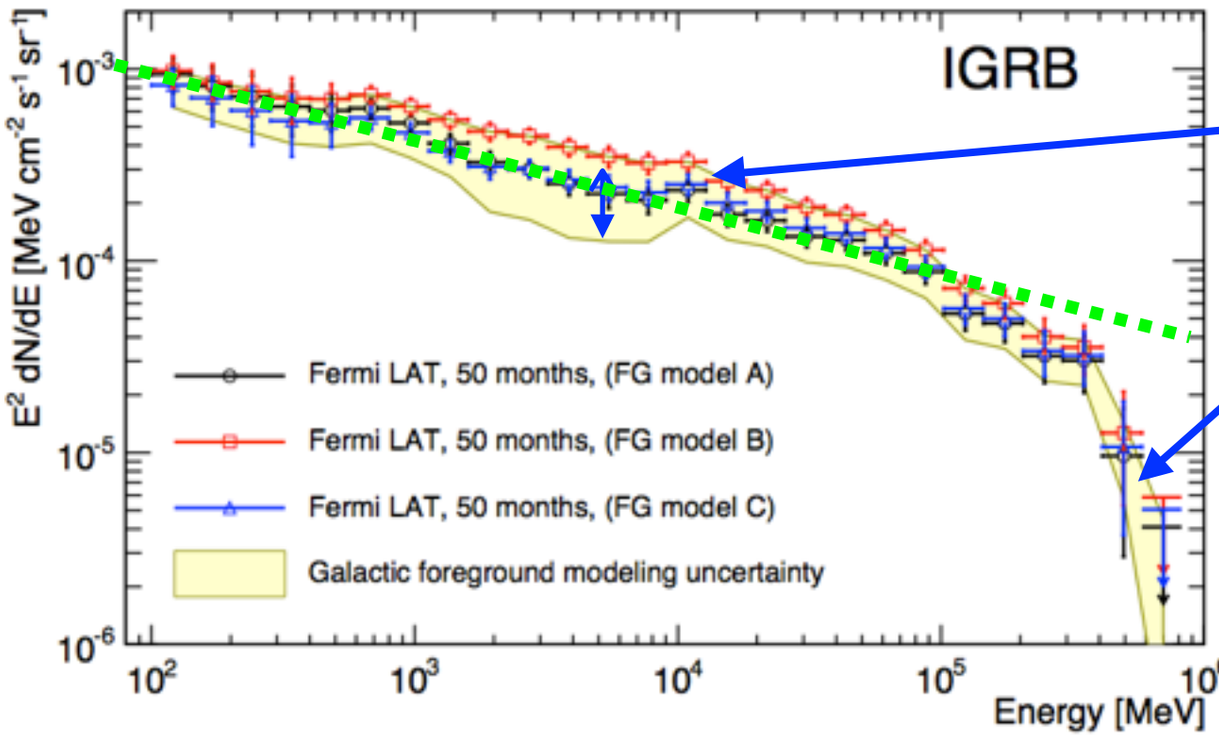

Systematic uncertainties on the GDE has been derived

Exponential cutoff.

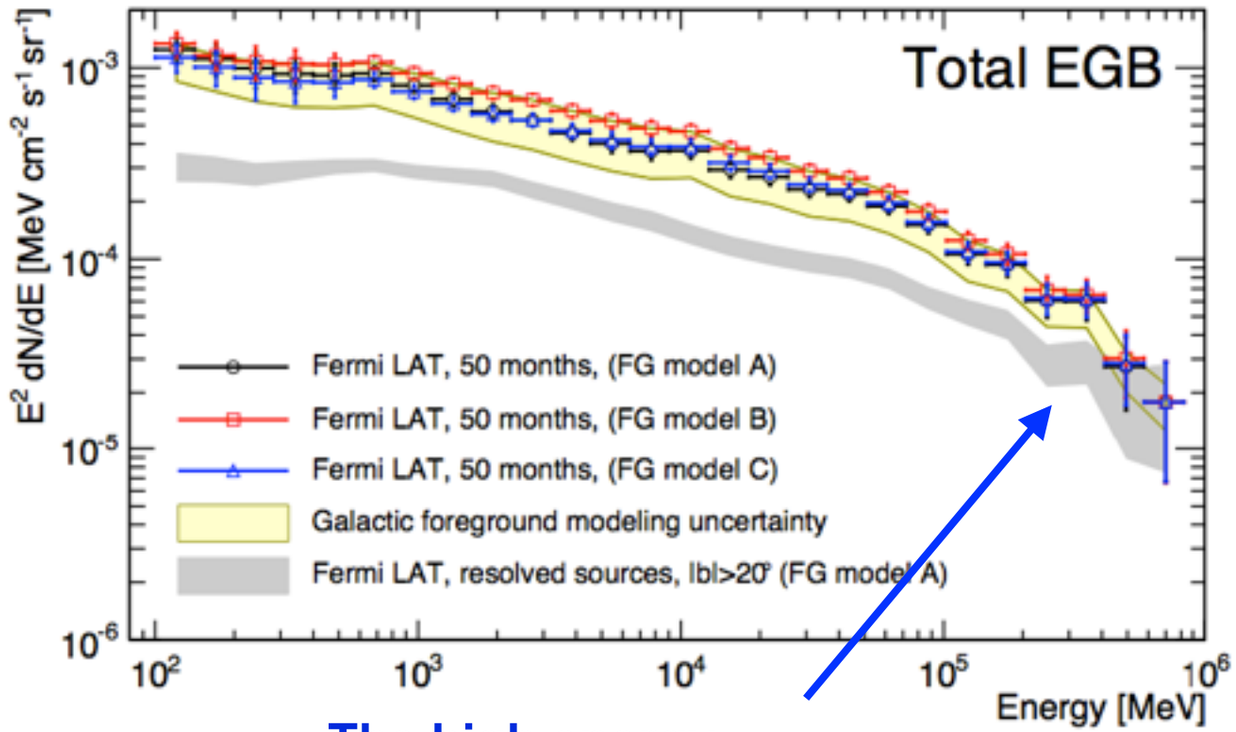

The high energy emission is dominated by resolved sources.

Ackermann et al. Arxiv 1410:3696 ApJ 2014

THE ORIGIN OF THE IGRB

UNRESOLVED SOURCES

AGN

Blazars (Bl Lac and FSRQ): 782 detected by Fermi-LAT in the 2FGL. 40%-60% IGRB. Abdo et al. 2010 ApJ 720 435, Ajello et al. 2012 ApJ 751 108, M. Ajello et al. 2014 ApJ 780 73. Di Mauro et al. 2014 ApJ 786 129.

MAGN: 20 detected by Fermi-LAT in the 1FGL and 2 FGL. 20-30% IGRB.Inoue 2011ApJ 733 66I, Di Mauro et al. 2014 *ApJ* 780 161

Pulsars: 160 in the 3FGL. Small contributions expected. few% IGRB. Siegal-Gaskins et al. 2010, Calore et al. 2012 Phys.Rev. D85 (2012), APJ Calore et al. 796 (2014) 1, 14.

Star-forming galaxies.

4%-23% of IGRB. Ackermann et al. 2012ApJ 755 164A, Chakraborty et al. ApJ 773 2013 104, Tamborra JCAP 9 2014 43.

DIFFUSE PROCESSES

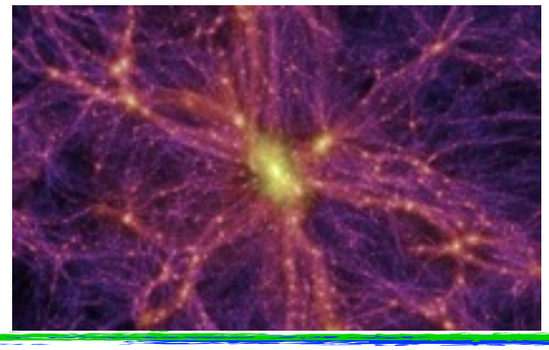

Dark matter: potential non negligible flux dependent on nature of DM, cross-section and DM distribution.

Intergalactic shocks: Widley varying predictions ranging from 1% to 100% (Loeb & Waxman 2000, Gabici & Blasi 2003, Zandanel et al. 2014)

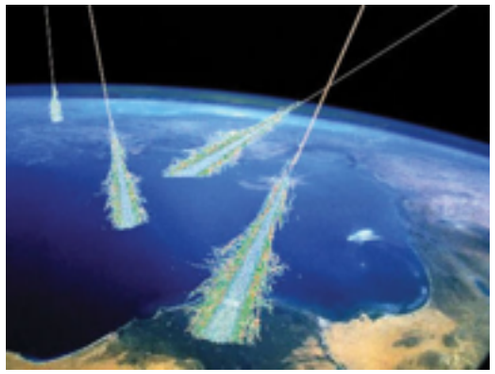

Interactions of UHE cosmic rays with the EBL: Dependent on evolution of CR sources, predictions varying from (Kalashev et al. 2009)

Extremely large Galacitc halo (Keshet et al 2004)

CR interaction in small solar system bodys (Moskalenko & Porter 2009)

GALACTIC PULSARS

- Pulsars are the most numerous Galactic population in Fermi catalogs (about 160 in the 3FGL).
- They are divided into young and millisecond sources.
- The young pulsars are highly concentrated in the Galactic plane therefore the contribution to the IGRB is mainly given by old sources.
- **The contribution to the IGRB is at most 1%.**

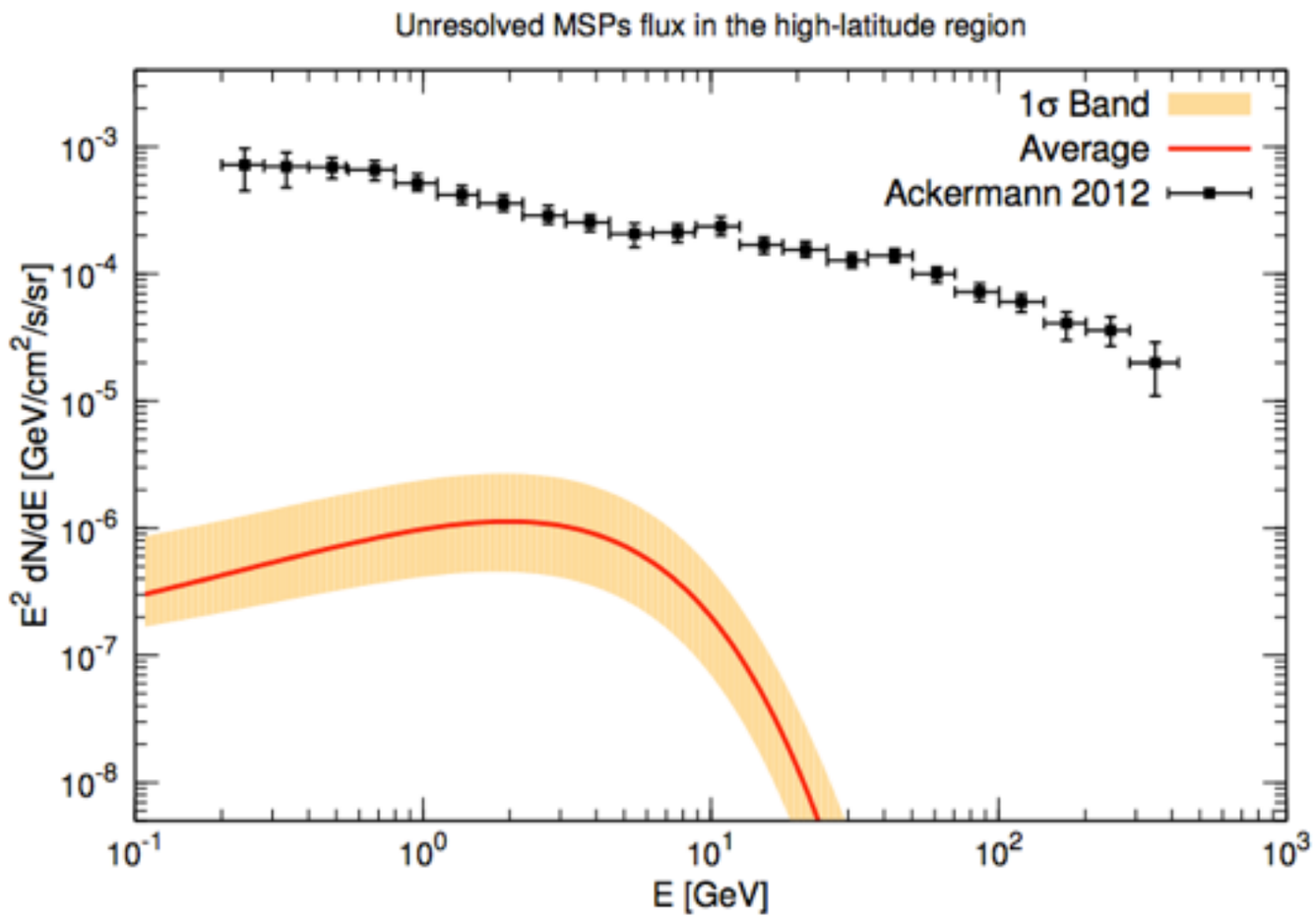

M. Di Mauro, et al. APJ 796 (2014) 1, 14.

Hooper, D. & Slatyer, T. R. 2013, Physics of the Dark Universe, 2, 118
Siegal-Gaskins et al. 2010,
Calore et al. 2012 Phys.Rev. D85 (2012), APJ

BLAZARS

BL LAC

BL LAC: Di Mauro et al. APJ, 786, 129

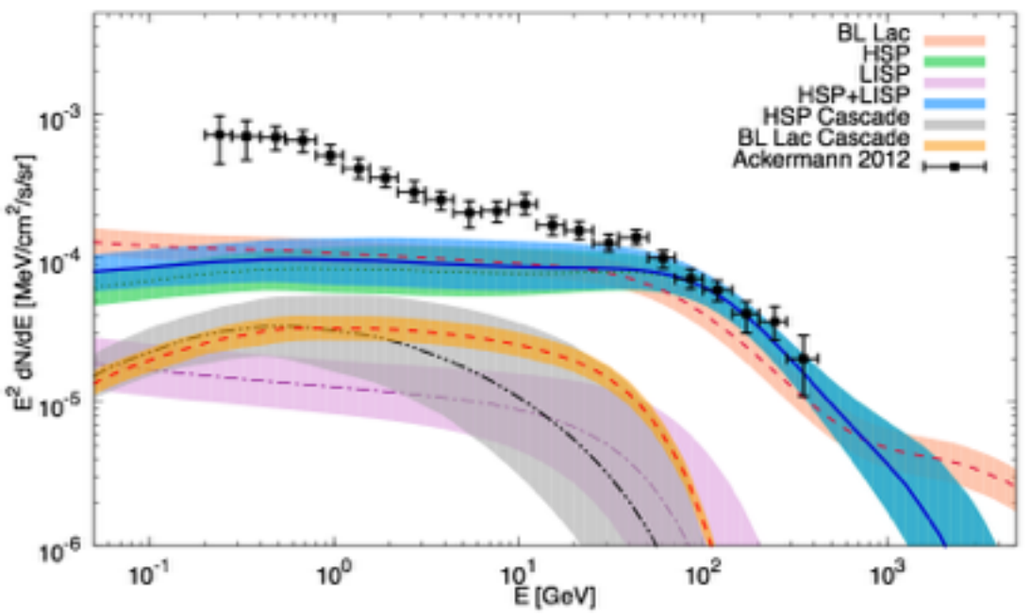

FSRQ

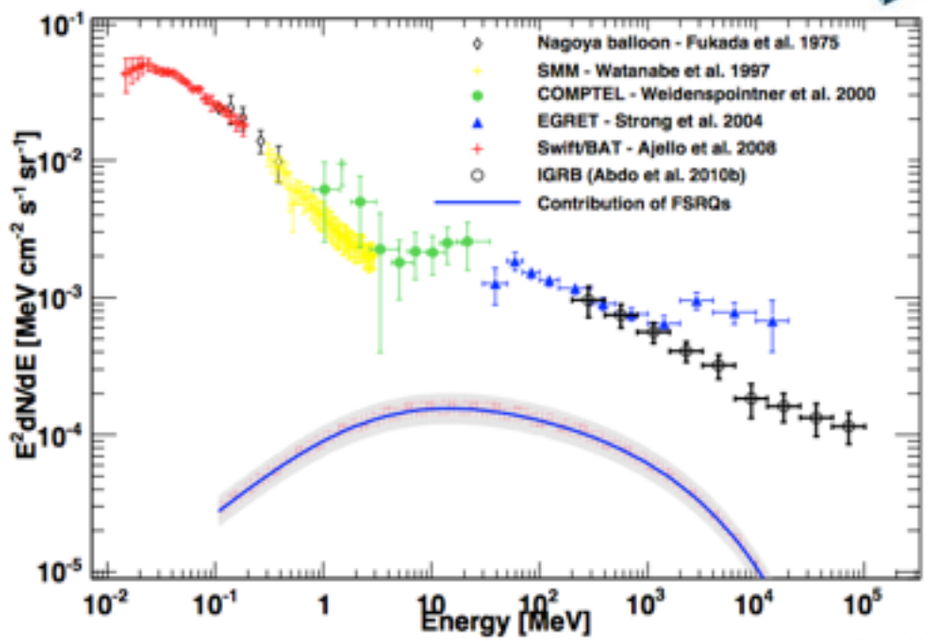

BLAZARS

Ajello et al. 2012
ApJ 751 108

- 40-60% of the IGRB
- The high energy part dominated by BL Lacs.
- FSRQs give their larger contribution in the low energy part of the spectrum.

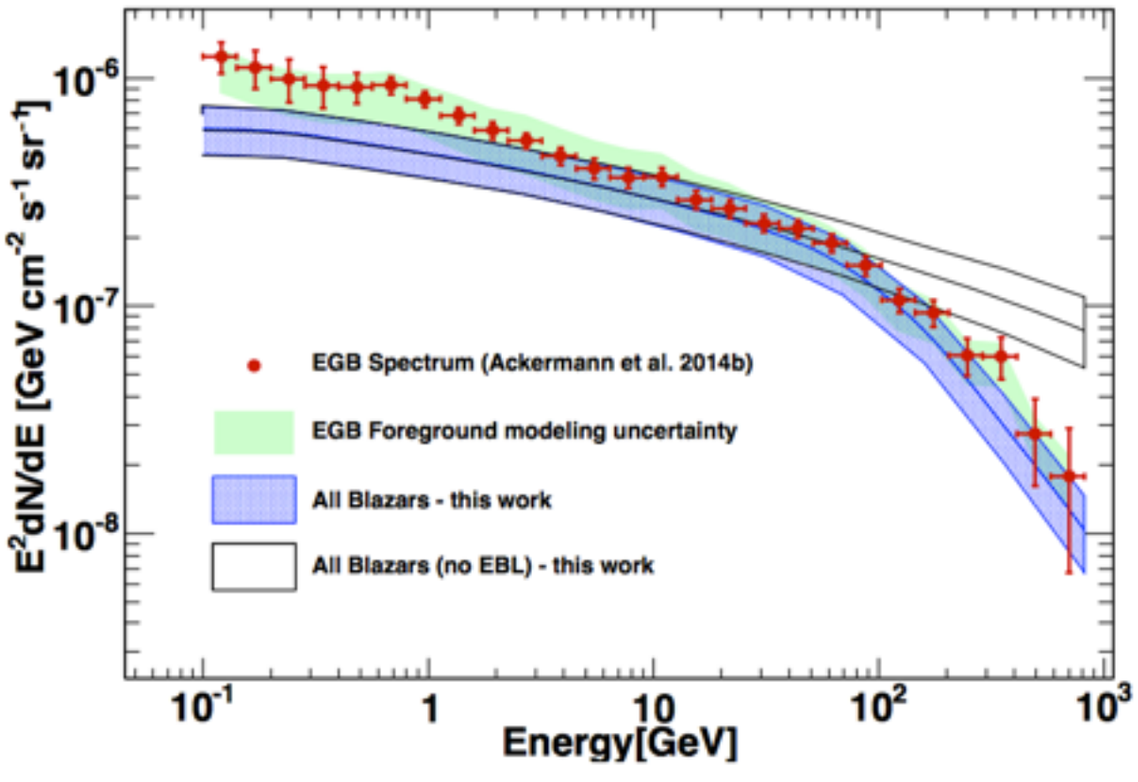

Ajello et al. Astrophys.J. 800 (2015) 2, L27

MAGN

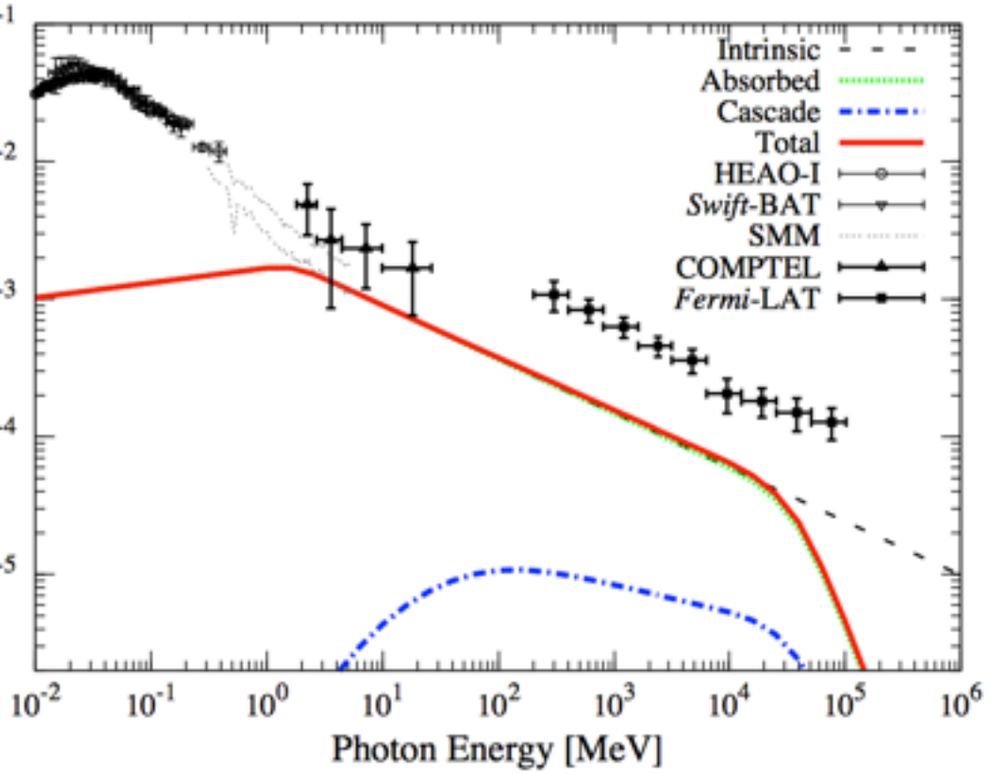

Inoue 2011 ApJ 733 66l

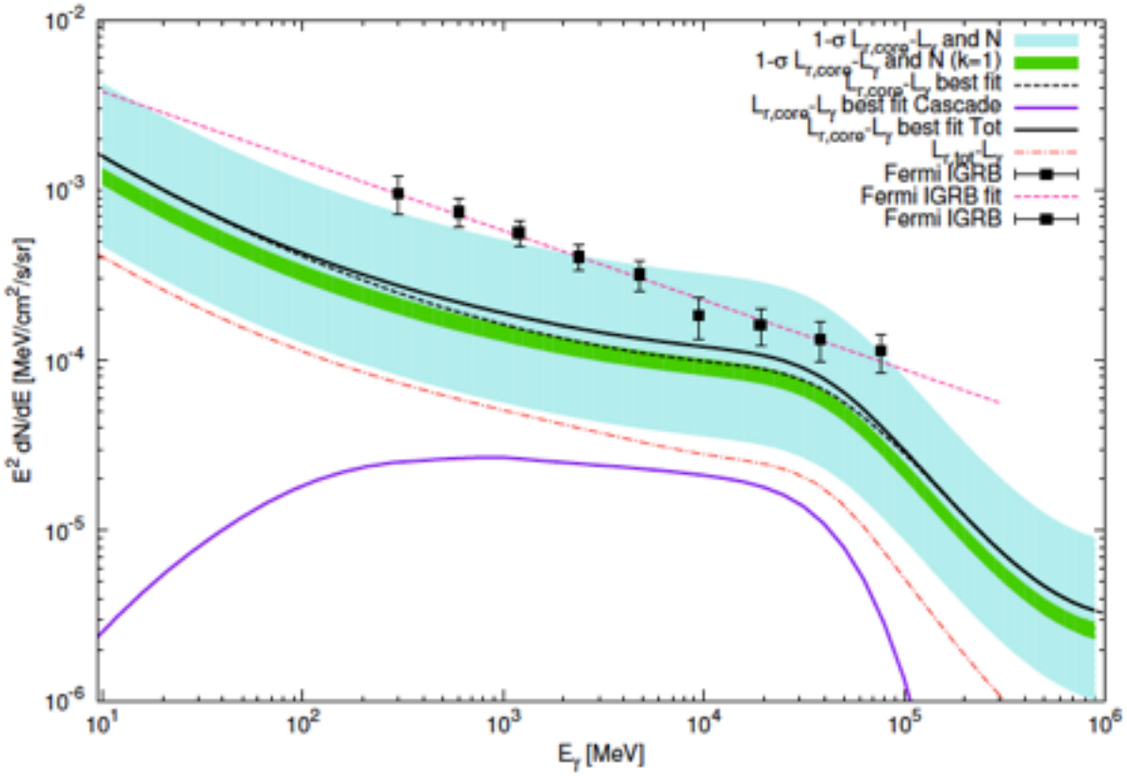

Di Mauro et al. 2014 *ApJ* 7

- **MAGN are AGN with the jets misaligned with respect to the line of sight.**
- **The sample of detected MAGN is quite small in Fermi catalogs (about 15 sources in the 3FGL).**
- **The unresolved contribution to the IGRB is derived using a correlation with radio band where MAGN are very numerous.**
- **MAGN contribute between 20-100% of the IGRB**

STAR FORMING GALAXIES

Ackermann 2012
ApJ...755..164A

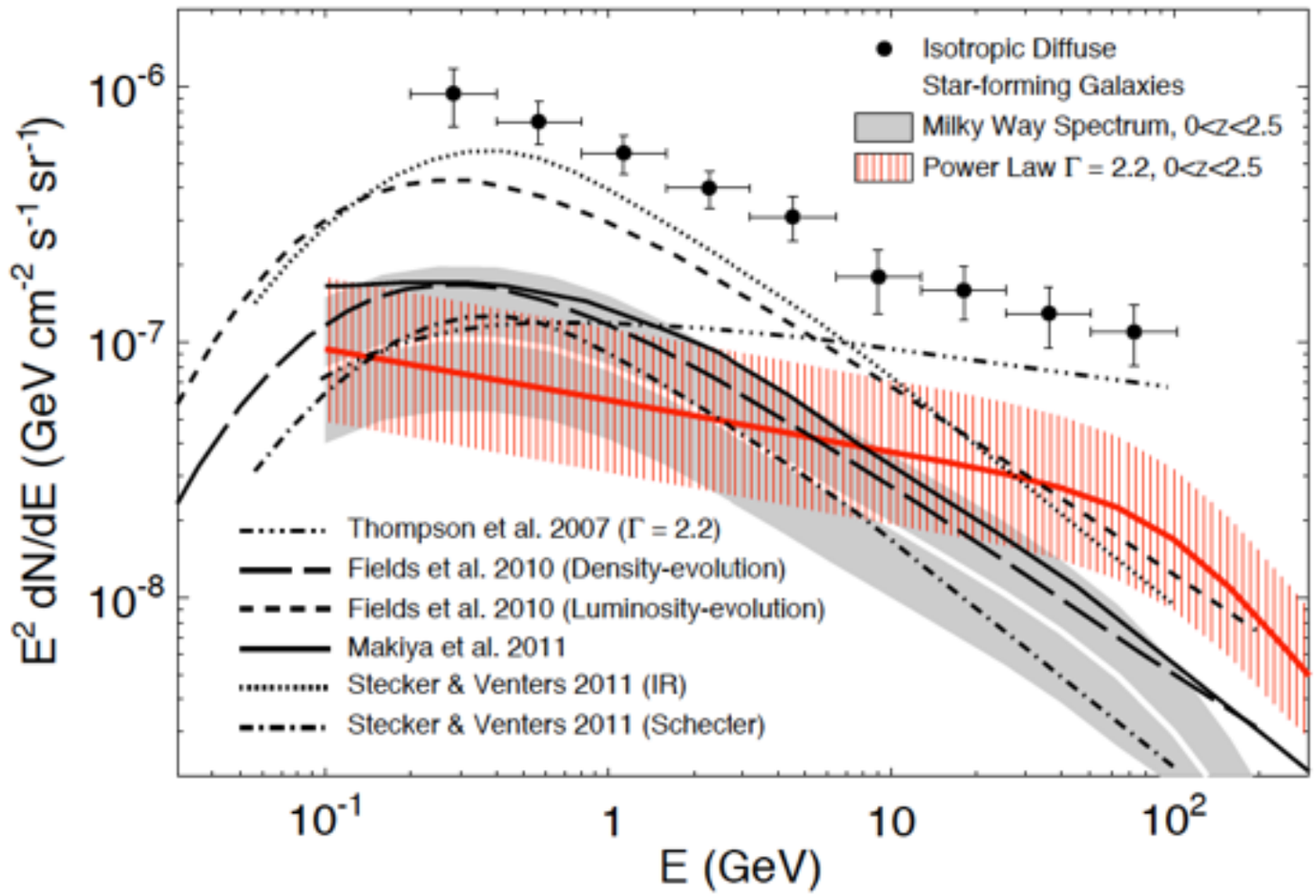

- **The sample of detected SFG is quite small in Fermi catalogs (about 5 sources in the 3FGL).**
- **The unresolved contribution to the IGRB is derived using a correlation with radio and infrared band where SFG are very numerous.**
- **SFGs contribute between 20-40% of the IGRB**

IGRB COMPOSITION OF IGRB AND EGB

IGRB composition with MW SF model

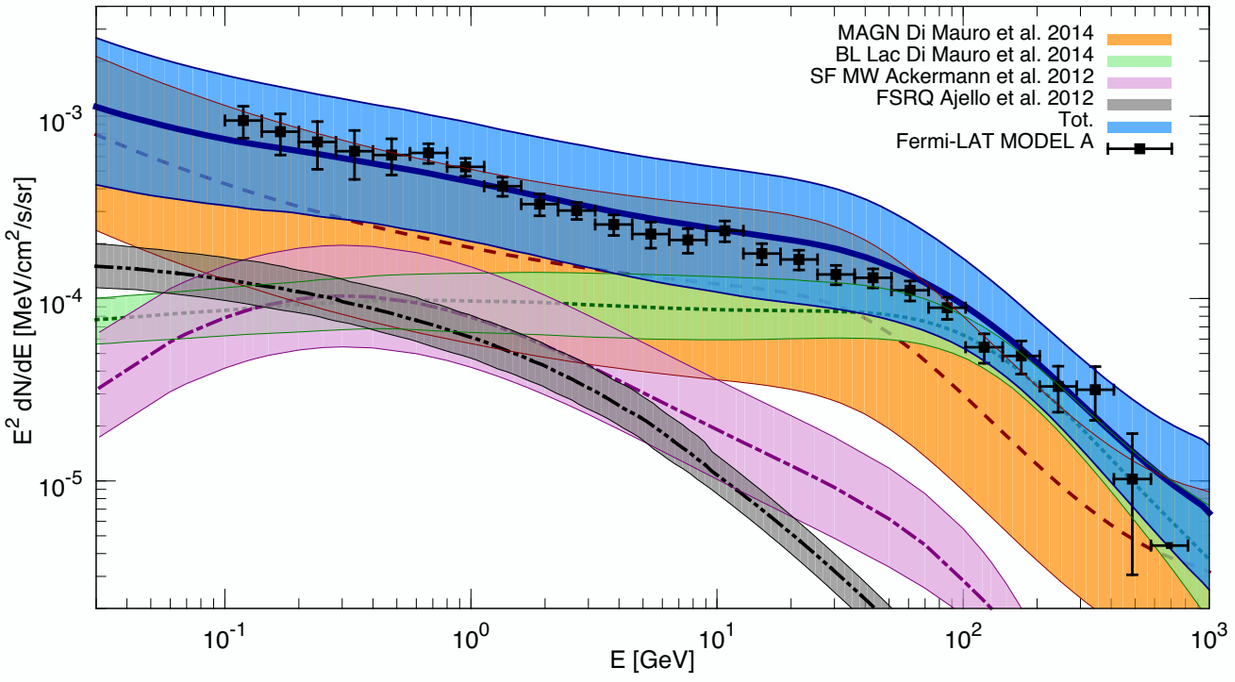

- **The IGRB and EGB spectra consistent with the superposition of gamma-ray emission from extragalactic sources.**
- **The room left to other exotic contribution as annihilation or decaying DM particles is really small.**

EGB

EGB composition with MW SF model

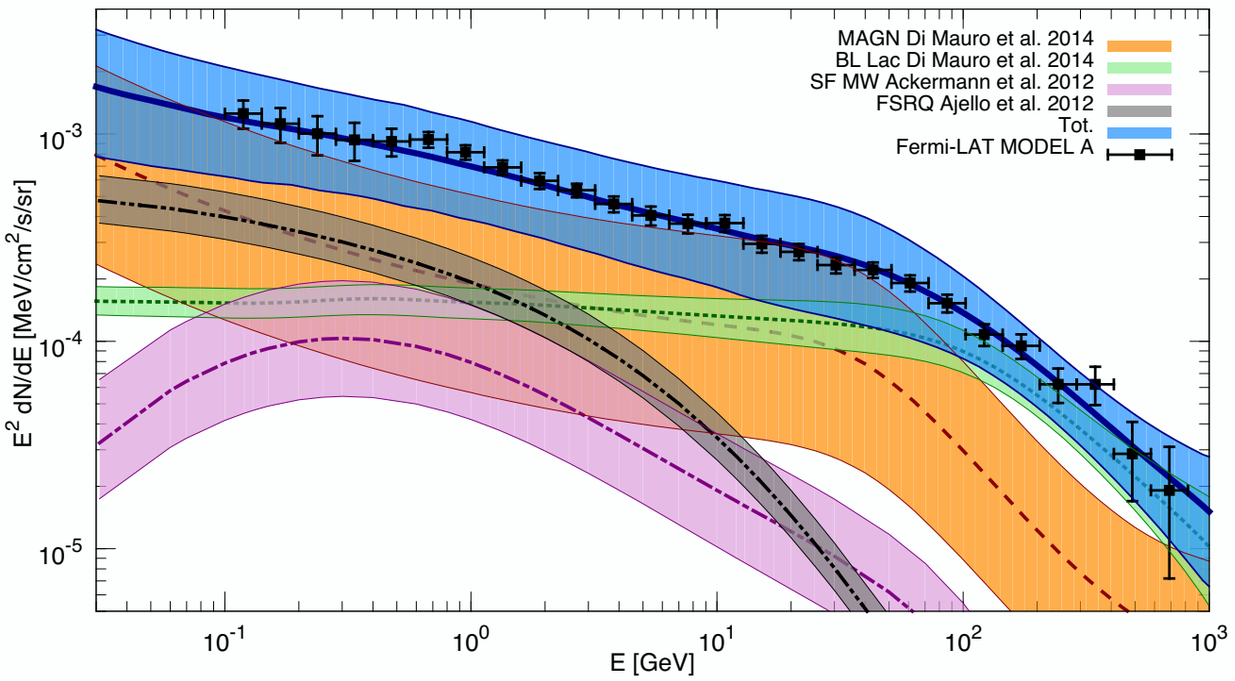

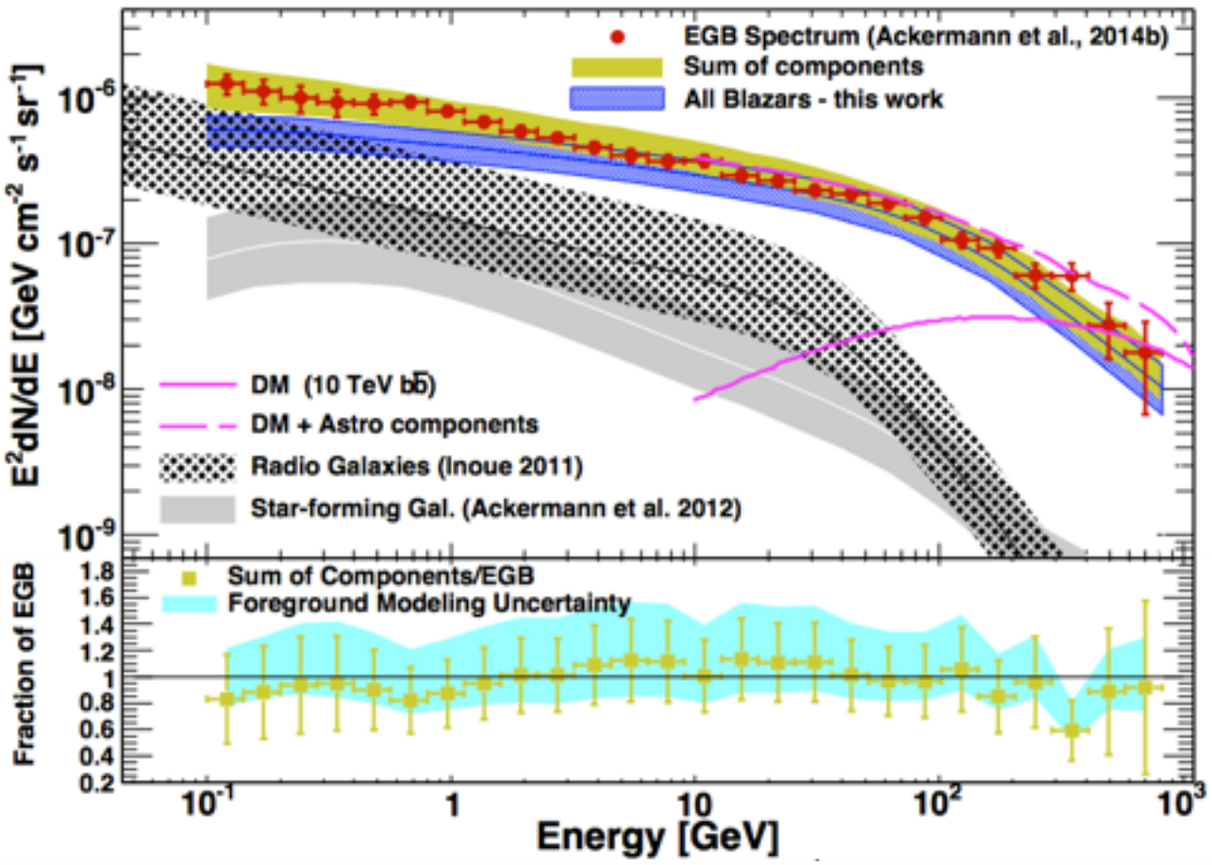

Di Mauro and Donato Phys.Rev. D91 (2015) 123001

Ajello et al. Astrophys.J. 800 (2015) 2, L27

Resolving the Extragalactic gamma-ray Background above 50 GeV with Fermi-LAT

Fermi-LAT Collaboration, Phys.Rev.Lett. 116 (2016) no.15, 151105

Photon fluctuation Analysis

- The photon fluctuation analysis **(PFA)** is a statistical tool that helps to derive the source count distribution **(dN/dS)** to the level where sources contribute on average 0.5 ph each.
- PFA has been successfully used in the past to predict the shape of the dN/dS below the sensitivity of ROSAT before Chandra and XMM, about one decade later, detected those faint sources.
- The analysis is performed by comparing the histogram of the pixel counts of the real sky with the ones obtained via Monte Carlo simulations and allows us to constrain the slope of the differential flux distribution below the threshold of the survey

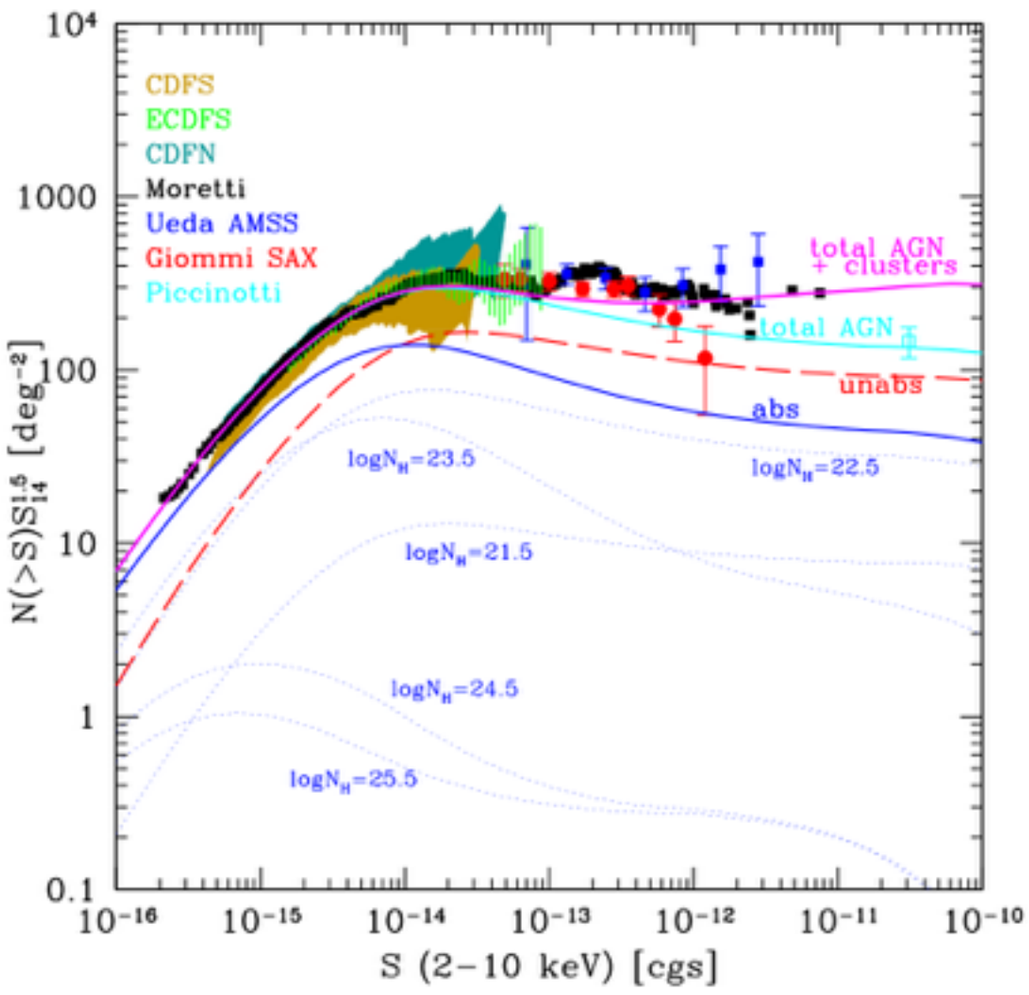

[15] Gilli et al. 2006

2FHL LogN-LogS

Why 2FHL ? Improvement delivered by Pass 8 enables study of the EBL, EGB, Galactic plane, and connects well to the TeV world

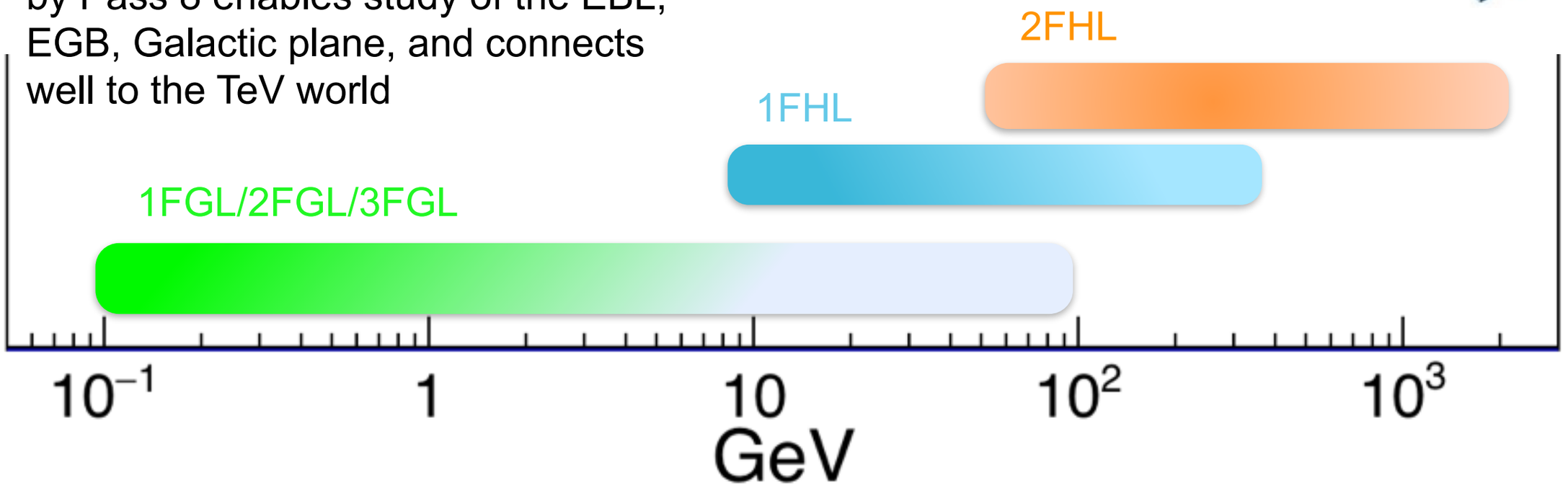

DETECTIONS

- **~360 sources**: 75% blazars, 11% Galactic sources, 14% unassociated
- At |b|>10° —> 70% BL Lacs and only 7 % No BL Lacs
- BCU type and unassociated sources —> 23%.
- This means that the fraction of likely blazars in the high-latitude 2FHL sample is 97%.

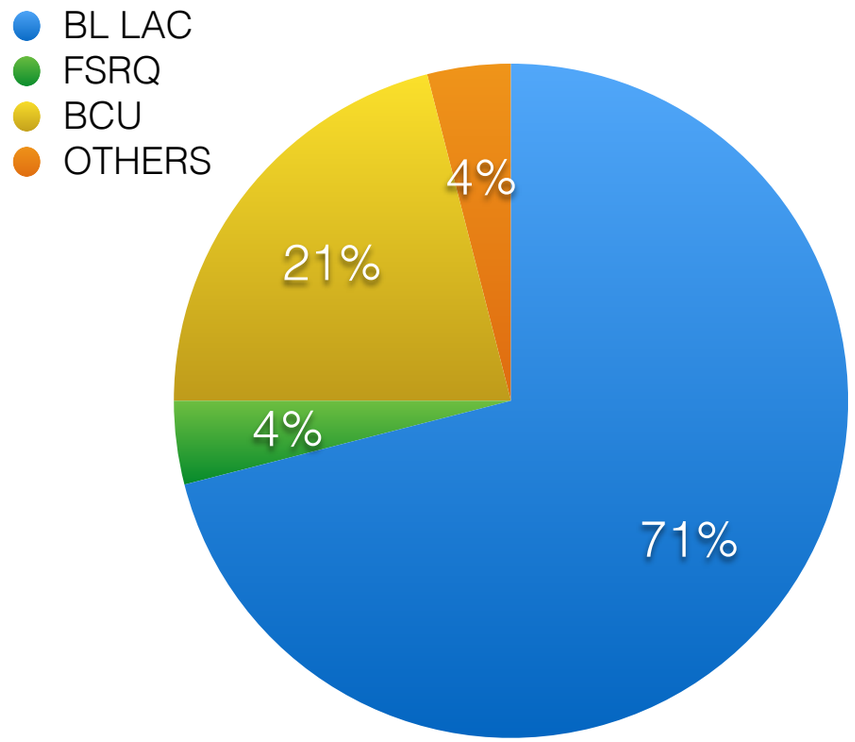

GAMMA-SKY FOR E>50 GeV

61,000 photons E > 50 GeV
18,000 photons E > 100 GeV ⟶ 1.5 ph/deg²
2,000 photons E > 500 GeV

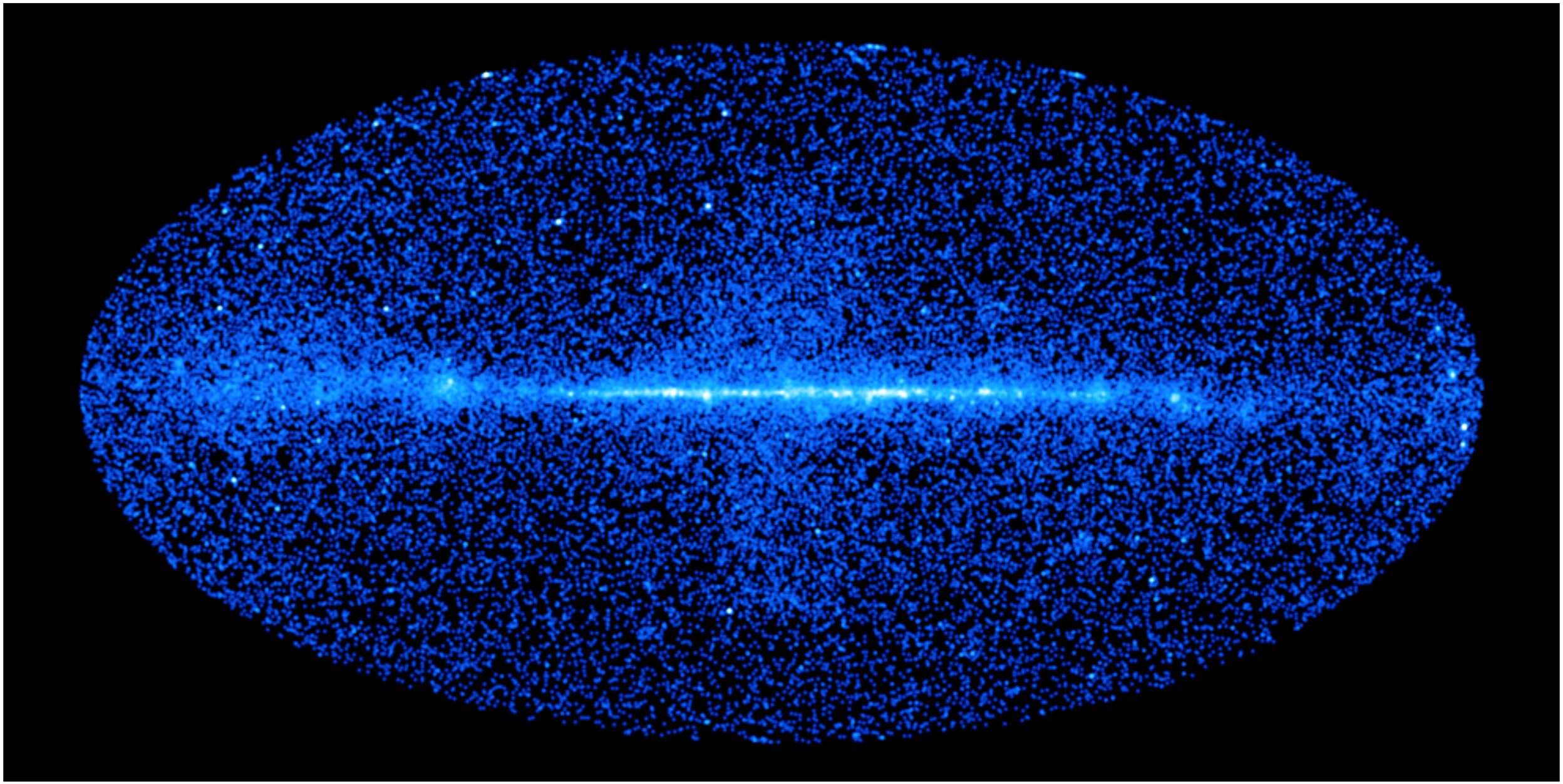

SIMULATED SKY MAP FOR E>50 GeV

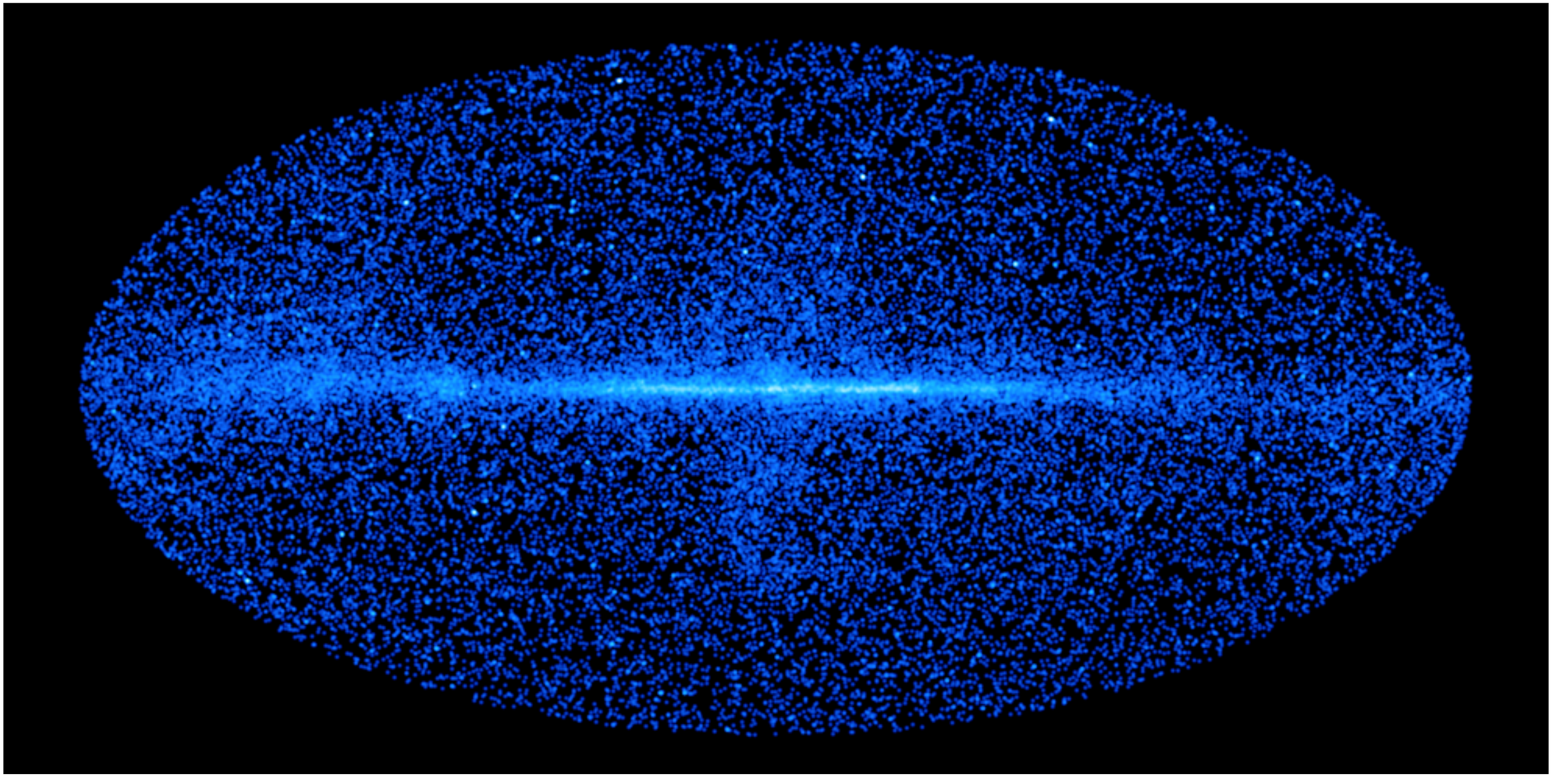

PHOTON FLUCTUATION ANALYSIS

- We employed the photon fluctuation analysis to derive the shape of the flux distribution below the sensitivity of the 2FHL catalog.
- Simulations with different value of the break and of the slope below the break have been tested.
- The flux distribution results to be consistent with a broken power law with a break in the range $\mathbf{S_b = [0.8,1.5] \cdot 10^{-11}}$ ph/cm^2/s and a slope above and below the break $\mathbf{\alpha_1 = 2.50}$ and $\mathbf{\alpha_2 = [1.6,1.75]}$
- The sensitivity of this method is around $\mathbf{1.3 \cdot 10^{-12}}$ **ph/cm^2/s**

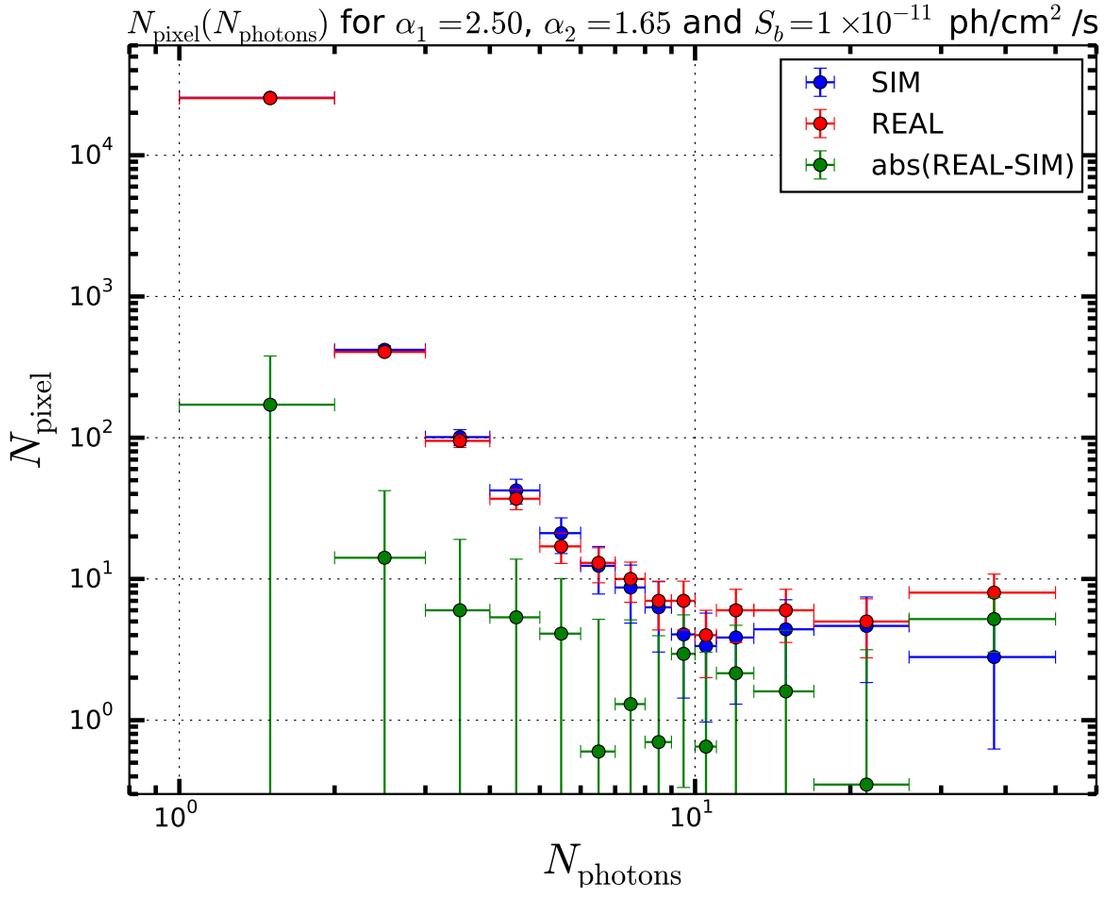

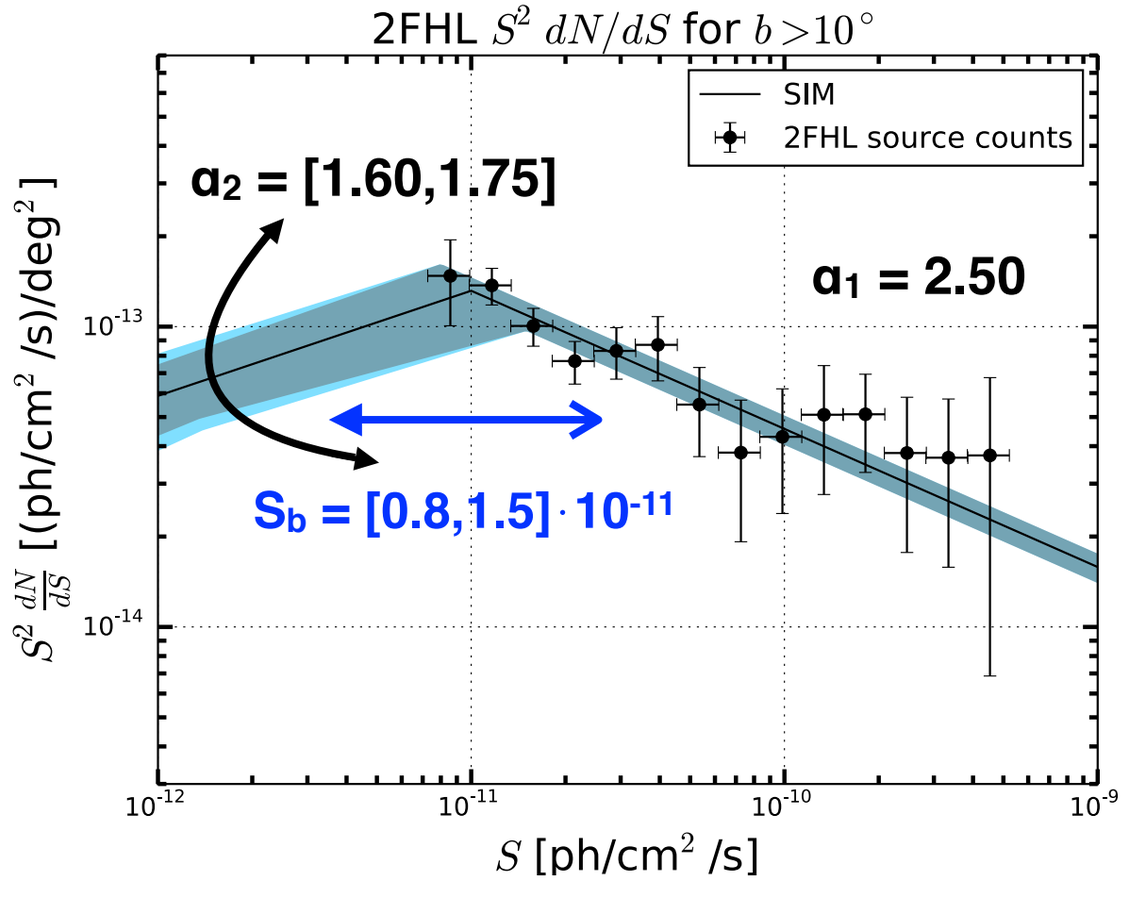

PHOTON FLUCTUATION ANALYSIS

- We employed the photon fluctuation analysis to derive the shape of the flux distribution below the sensitivity of the 2FHL catalog.
- Simulations with different value of the break and of the slope below the break have been tested.
- The flux distribution results to be consistent with a broken power law with a break in the range $\mathbf{S_b = [0.8,1.5] \cdot 10^{-11}}$ ph/cm^2/s and a slope above and below the break $\mathbf{\alpha_1 = 2.50}$ and $\mathbf{\alpha_2 = [1.6,1.75]}$
- The sensitivity of this method is around $\mathbf{1.3 \cdot 10^{-12}}$ **ph/cm^2/s**

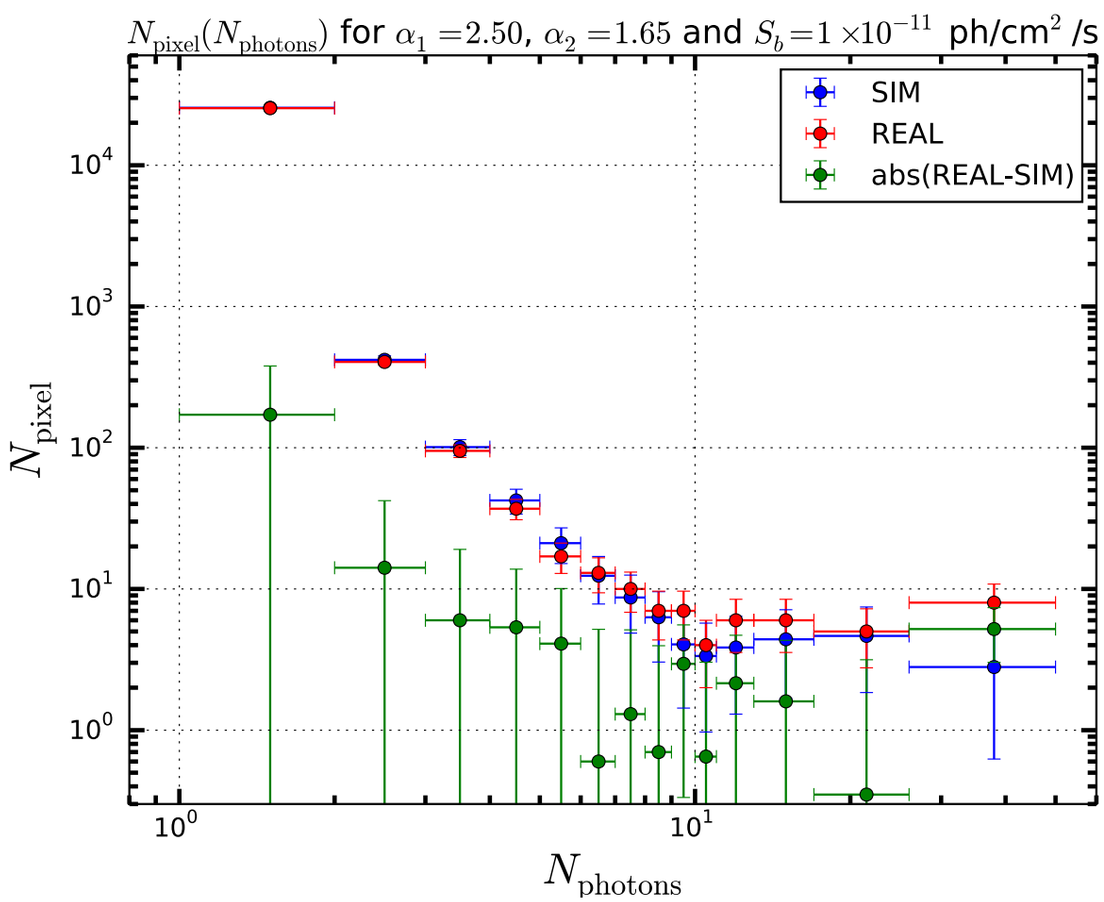

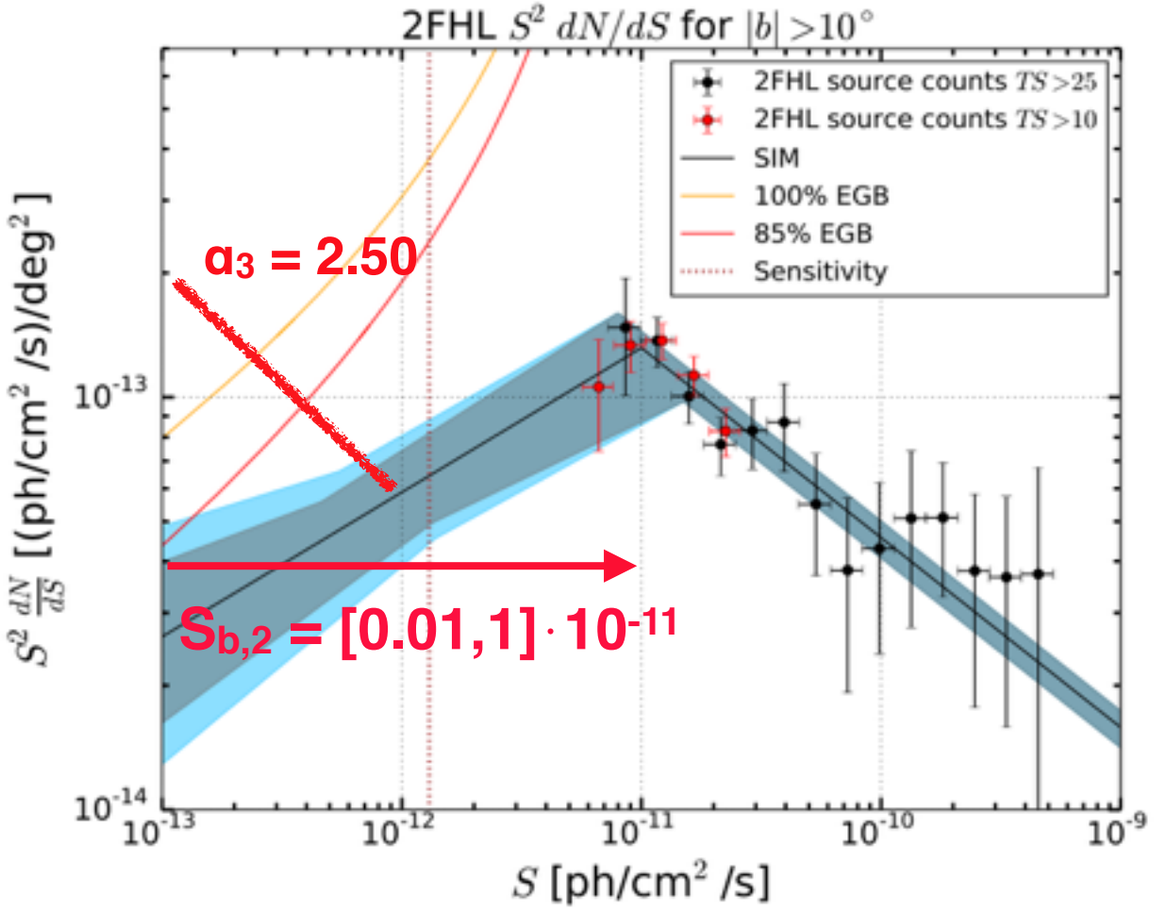

Detection Efficiency

$$\omega(S^i \in [S^i_{\rm min}, S^i_{\rm max}]) = \frac{N^i_{\rm meas}}{N^i_{\rm true}}$$

The efficiency starts to deviate from one for F < 1.3-1.5·10^{-11} ph/cm^2/s

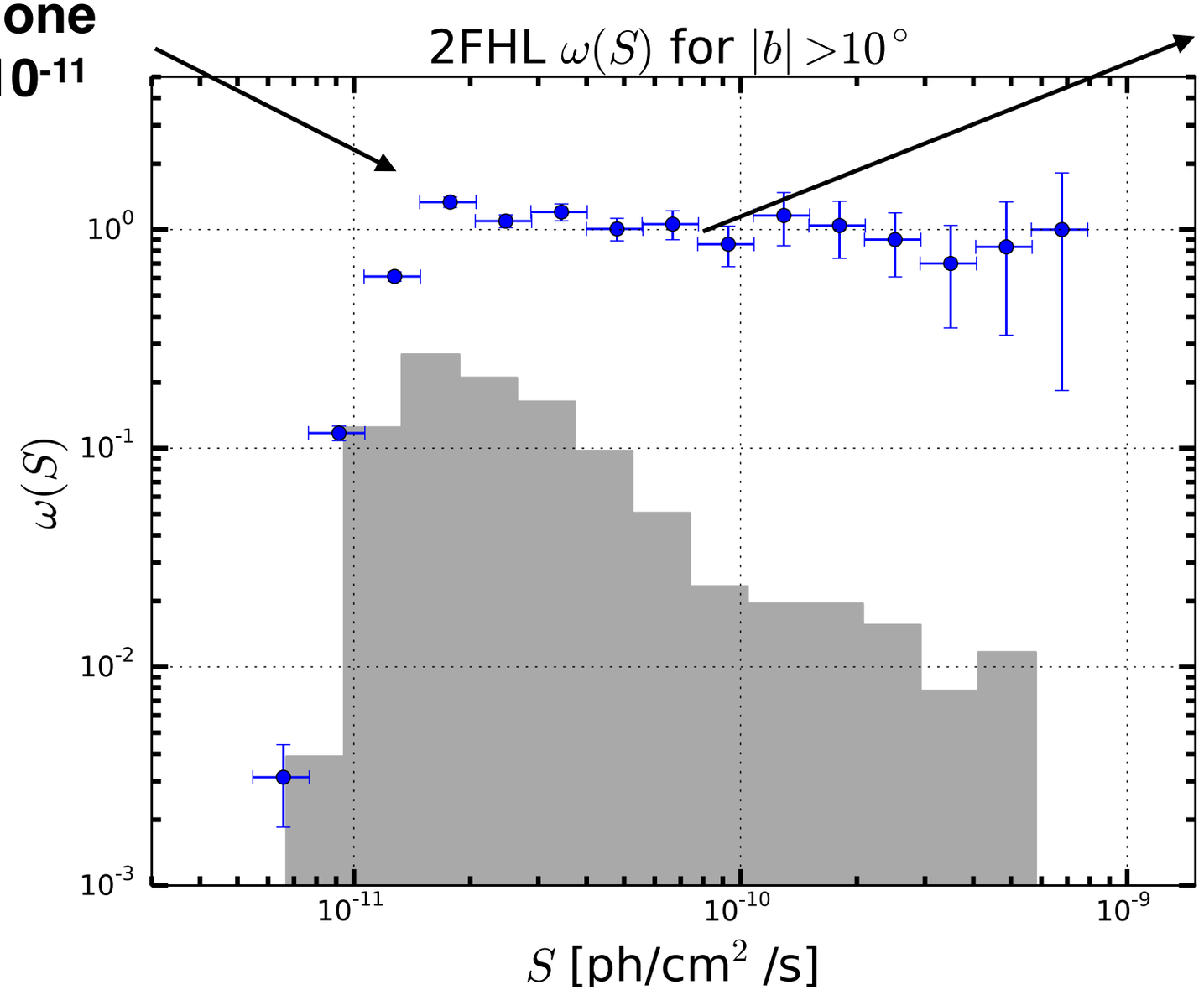

Efficiency~1 for bright sources

CORRECTED LOGN-LOGS

- **A fit to the corrected LogN-LogS of the 2FHL gives α = 2.49 ± 0.12!**
- **This is the result of 10 simulations.**
- **The band takes into account the uncertainty of the flux distribution given by the photon fluctuation analysis.**

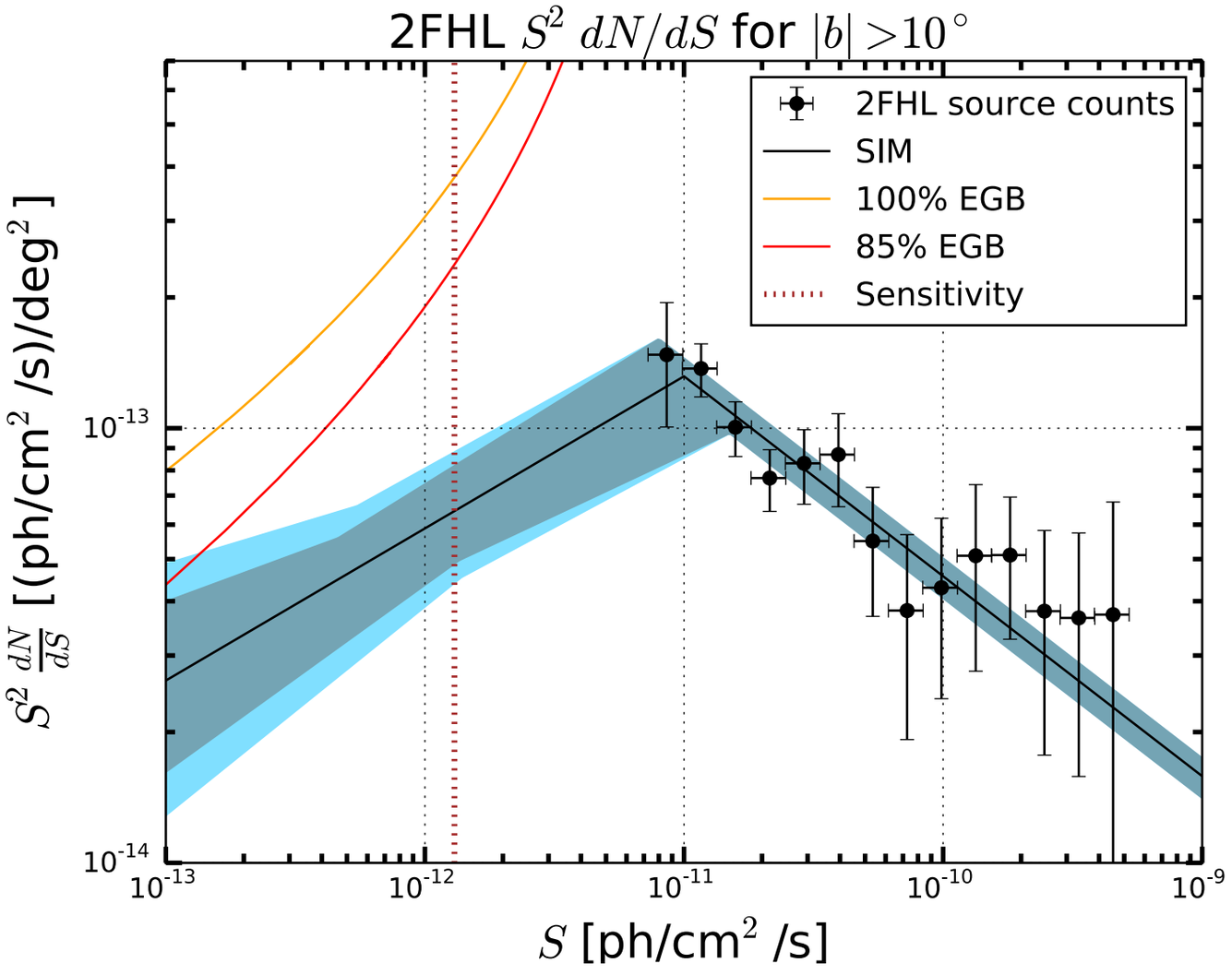

The orange and red curves indicate where 85% and 100% of the EGB intensity above 50 GeV would be produced when extrapolating the flux distribution below the break with different values of faint-end slope, α_2.

Additional confirming tests for the break

1) Number of detected sources

- The number of sources detected at |b|>20 deg in the 2FHL is 253
- Our best fit model predicts 271 ± 18 detected sources —> Consistent with 2FHL
- Taking $S_b = 5 \cdot 10^{-12}$ ph/cm²/s and a slope above and below the break $\alpha_1 = 2.50$ and $\alpha_2 = 1.10$ we find 318 ± 20 detected sources.

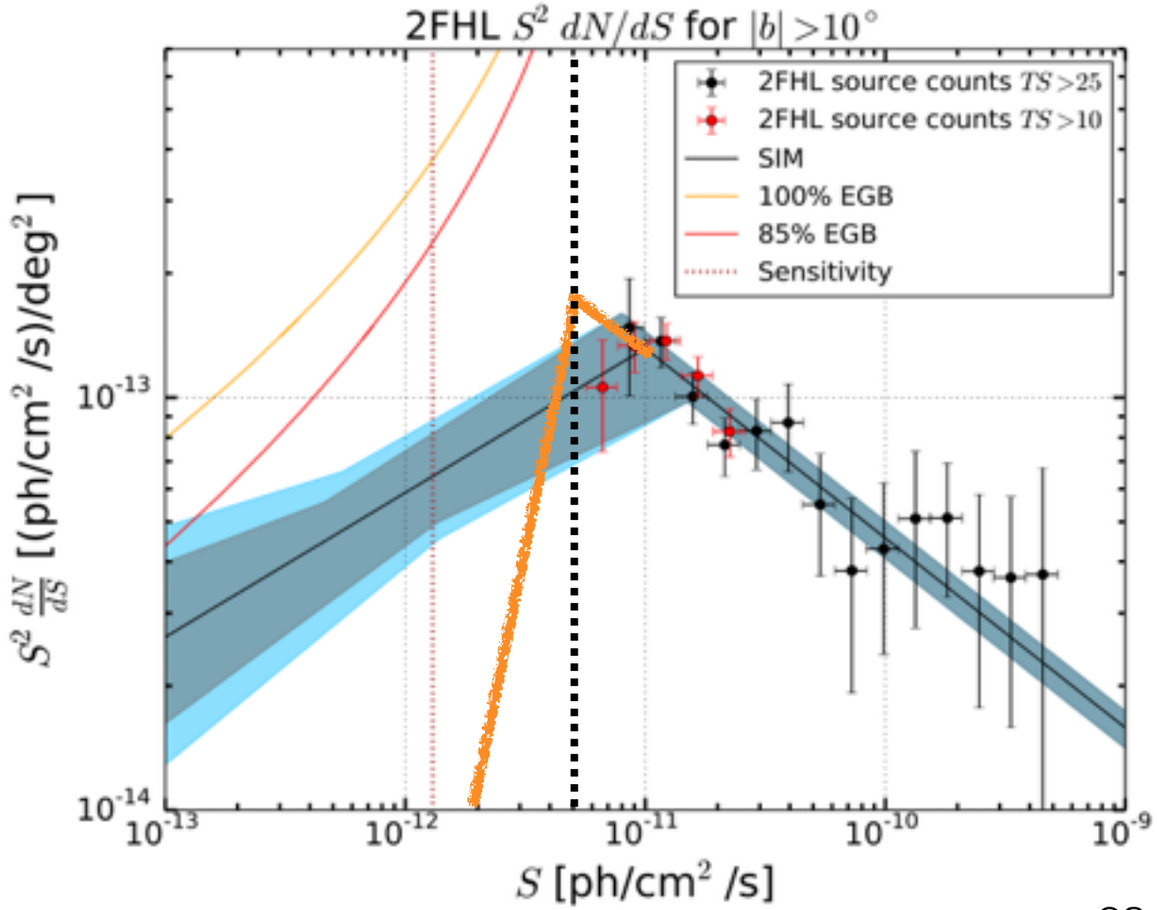

Additional confirming tests for the break

1) Number of detected sources

- The number of sources detected at |b|>20 deg in the 2FHL is 253
- Our best fit model predicts 271 ± 18 detected sources —> Consistent with 2FHL
- Taking $S_b = 5 \cdot 10^{-12}$ ph/cm²/s and a slope above and below the break $\alpha_1 = 2.50$ and $\alpha_2 = 1.10$ we find 318 ± 20 detected sources.

2) TS>10 sources.

- We have derived the detection efficiency for TS>10 sources.
- Then we have calculate the intrinsic LogN-LogS adding one low flux point to the previous dN/ds.

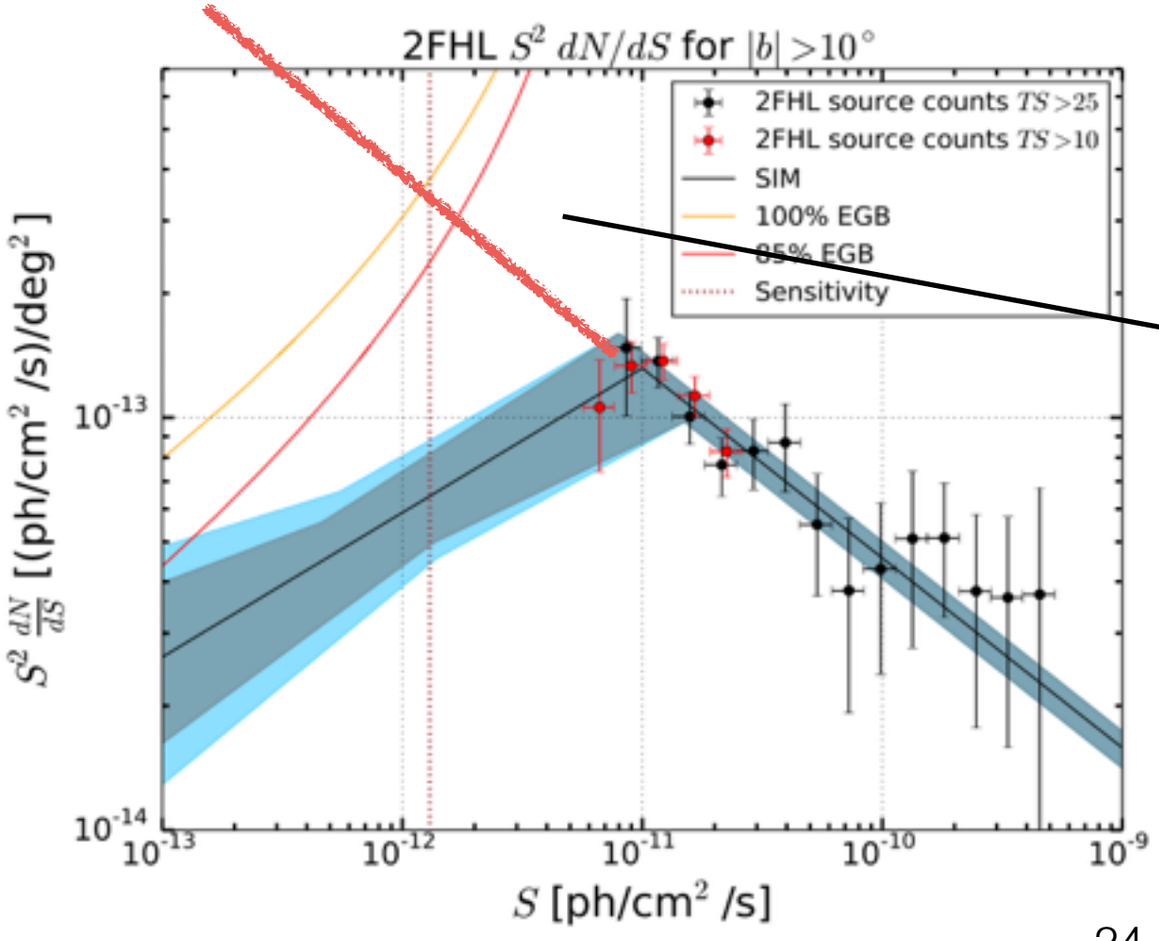

3) The Euclidean distribution below the 2FHL cat threshold is constrained by the EGB.

CUMULATIVE SOURCE COUNT DISTRIBUTION

- **The observed cumulative source count distribution is consistent with theoretical prediction of Di Mauro et al. 2014, Giommi et al. 2015 and Ajello et al. 2015.**
- **The expected sensitivity of CTA is just below the Fermi-LAT sensitivity.**
- **We have already resolved almost all the gamma-ray sky CTA will observe!!**

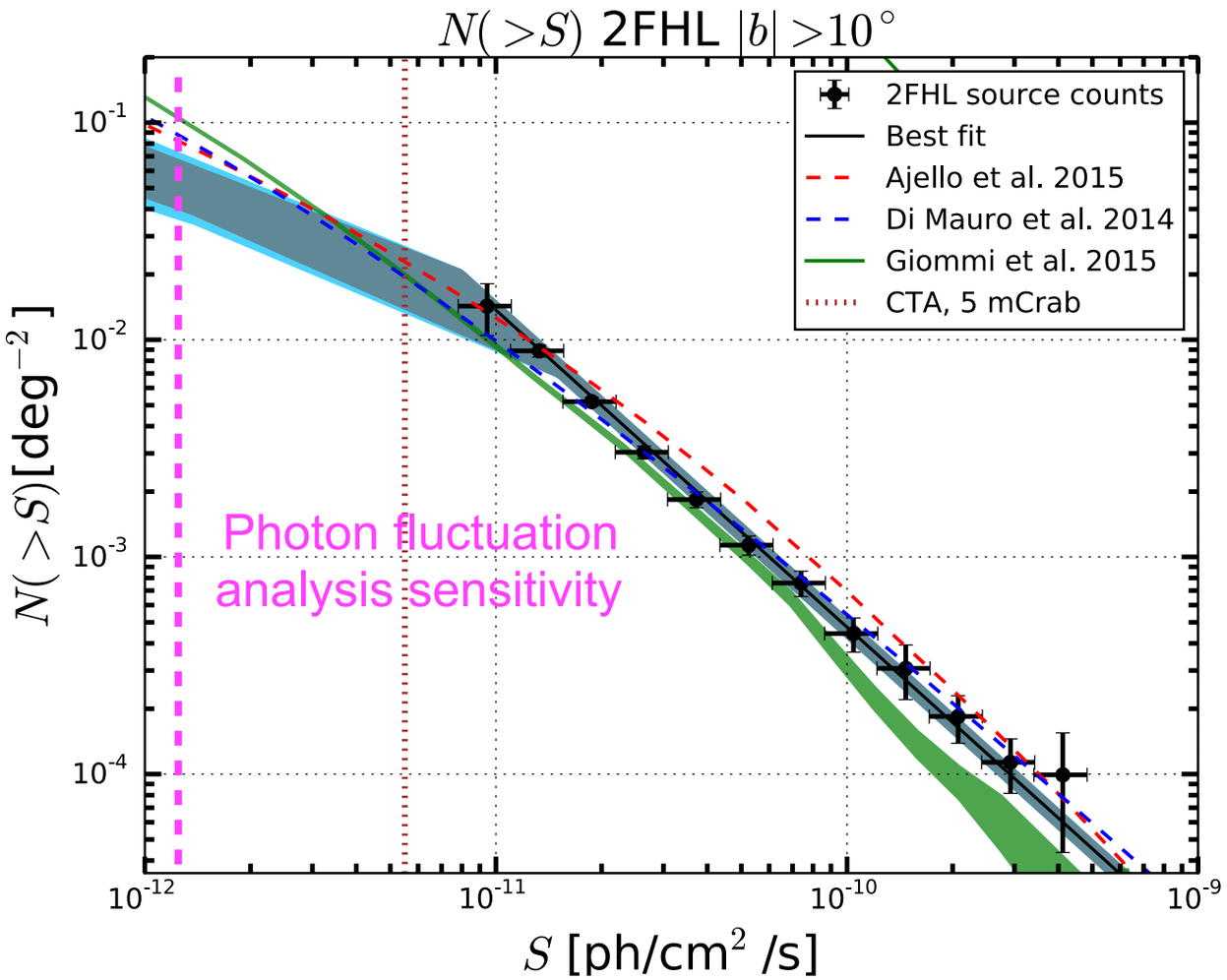

- **The CTA sensitivity is reachable in 240 hours in the most sensitive pointing strategy.**
- **At these fluxes the source density is 0.0194±0.0044 deg^{-2}, which translates into the serendipitous detection of 200 ± 45 sources in a field of one quarter of the entire sky**

CONTRIBUTION TO THE IGRB AND ANISOTROPY

$$I = \int_{S_{\rm min}}^{S_{\rm max}} S \, \frac{dN}{dS} dS \qquad [\mathrm{ph\,cm^{-2}\,s^{-1}\,sr^{-1}}]$$

EGB —> $(2.40 \pm 0.30) \cdot 10^{-9}$ ph/cm^2/s/sr

$2.07^{+0.40}_{-0.35} \cdot 10^{-9}$ ph/cm^2/s/sr

86%$^{+16}_{-14}$ of the EGB

$$C_P = \int_0^{\infty} (1 - \omega(S))\, S^2 \frac{dN}{dS} dS \qquad [(\mathrm{ph/cm^2/s})^2\ \mathrm{sr}^{-1}]$$

$C_p(E > 50\ \mathrm{GeV}) = 9.4^{+1.0}_{-1.5}$

10^{-22} (ph/cm^2/s)^2/sr

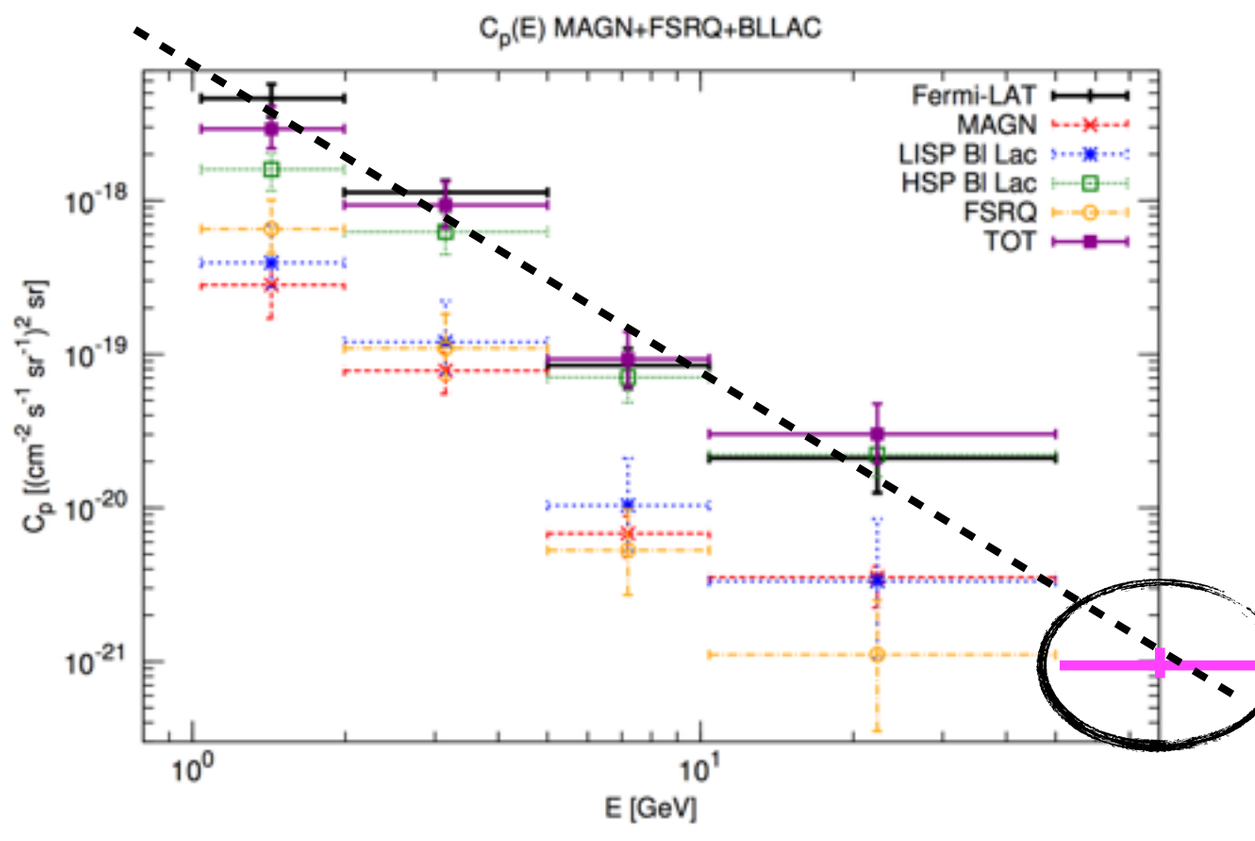

Di Mauro et al. 2014

CONCLUSIONS

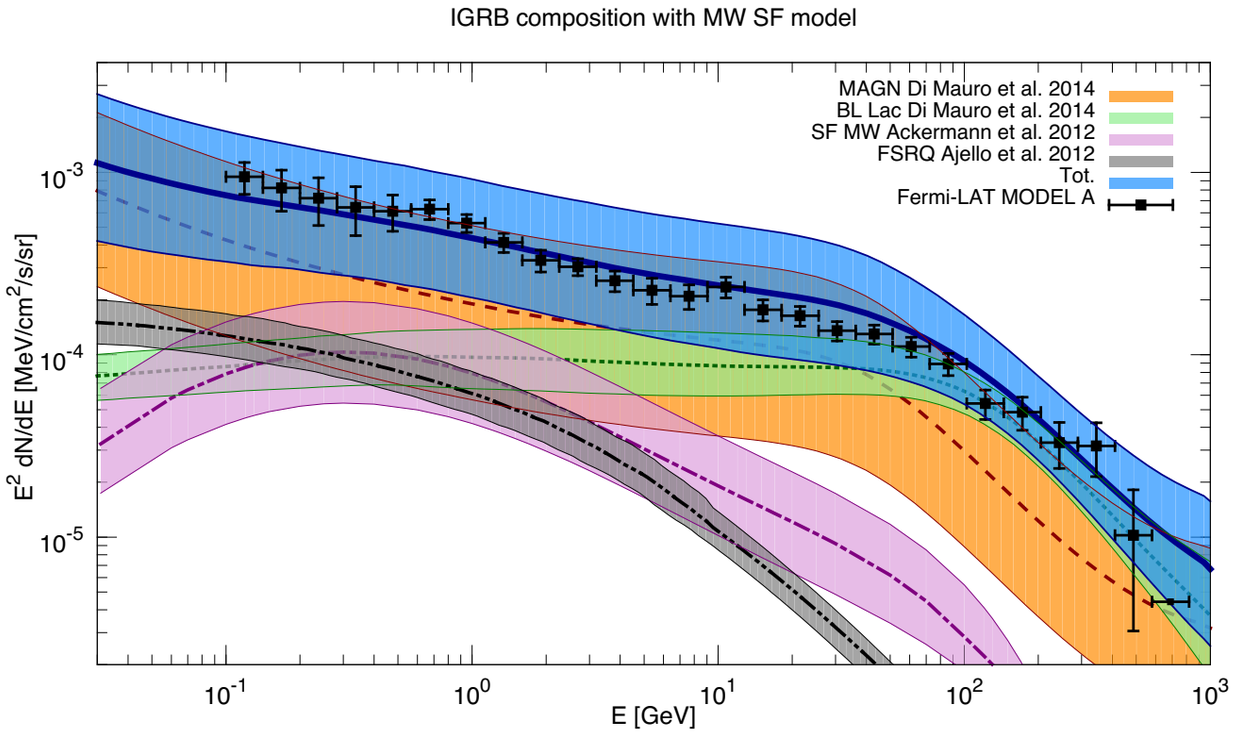

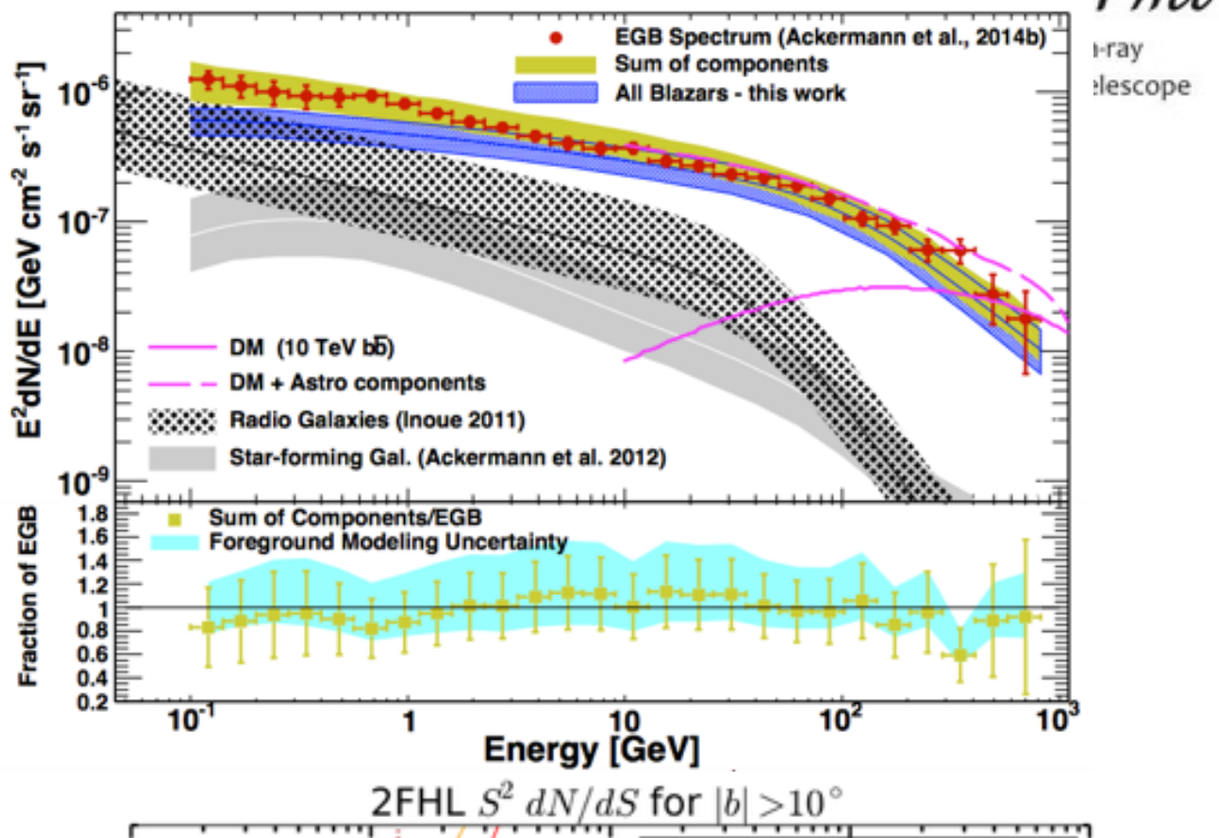

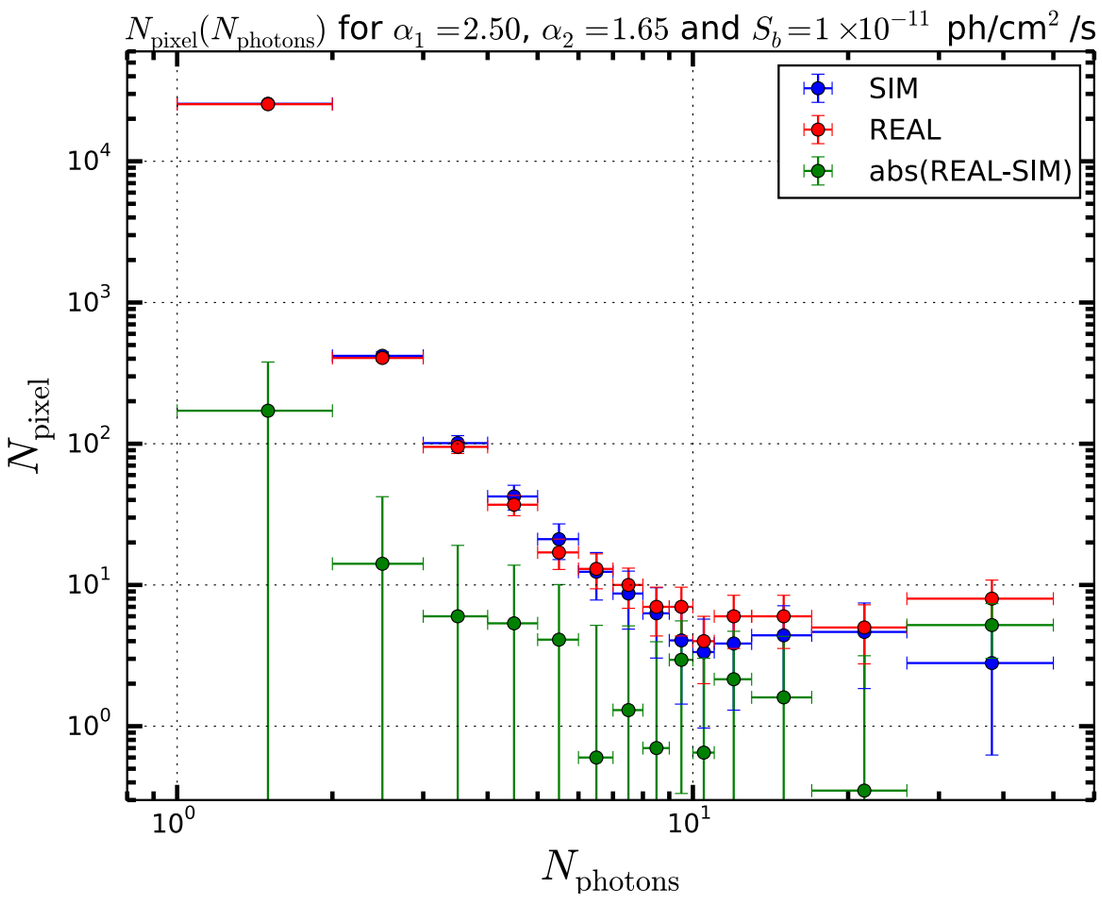

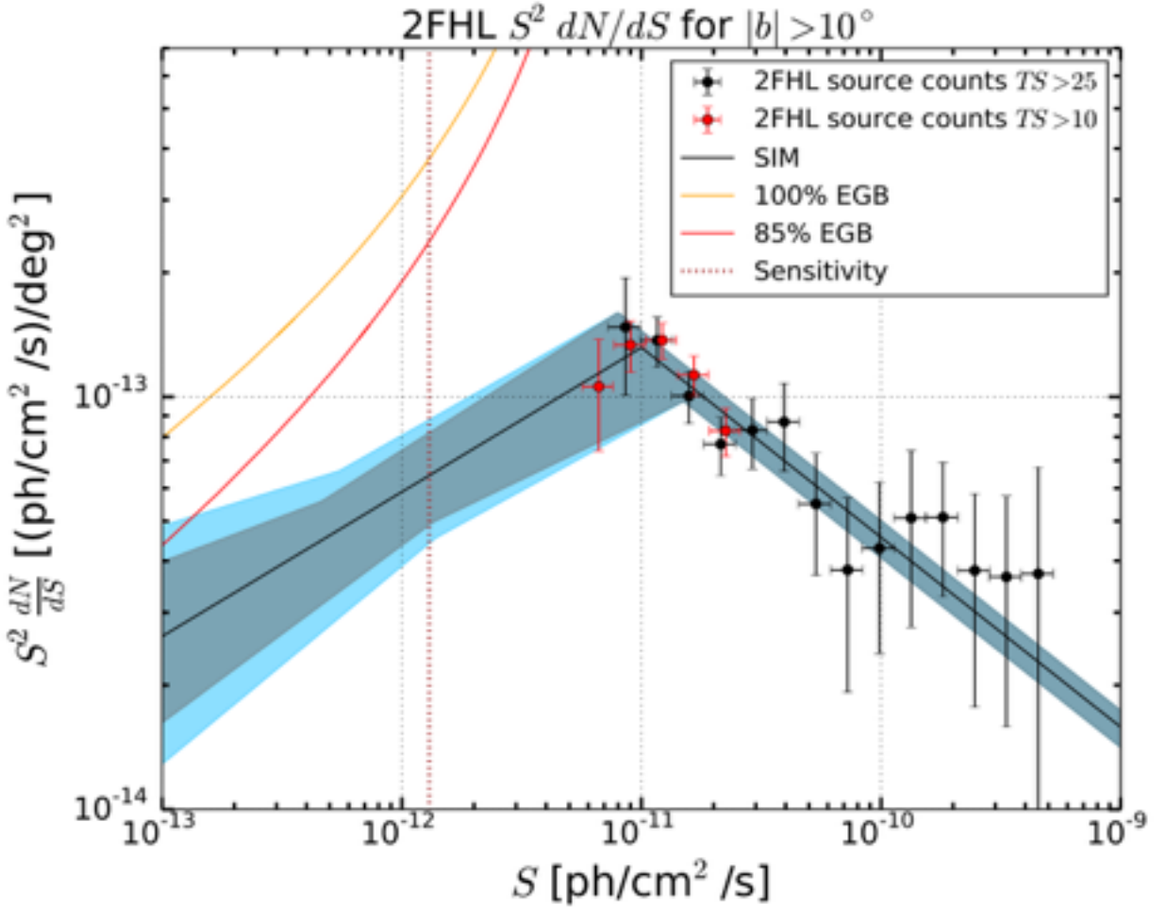

BACKUP

CONCLUSIONS

- **IGRB: unresolved gamma-ray emission from AGN and SFGs.**
- **Dedicated analysis for E>50 GeV using the 2FHL catalog.**
- **Taking into account realistic simulations and the photon fluctuation analysis we infer that dN/dS is a broken power-law.**
- **The photon fluctuation: lower a factor of 8 the sensitivity with respect to the 2FHL cat.**
- **The Fermi-LAT sensitivity is just above the expected sensitivity of CTA.**
- **We explain almost all the IGRB at E=[0.1,820] GeV and for E=[50,2000] GeV with AGN and SFGs.**
- **Small room is left to other exotic channels as gamma rays produced from annihilation or decay of DM particles and emission from other diffuse processes as interaction of UHECRs with EBL.**

STEP 1

- **Sources with a dN/dS slope of 2.34 and a photon index of 3.2 ± 0.4**
- **Extended isotropic diffuse using: isotropic_source_4years_P8V3_extended.txt**
- **Galactic diffuse using: gll_iem_v05_rev1.fit**

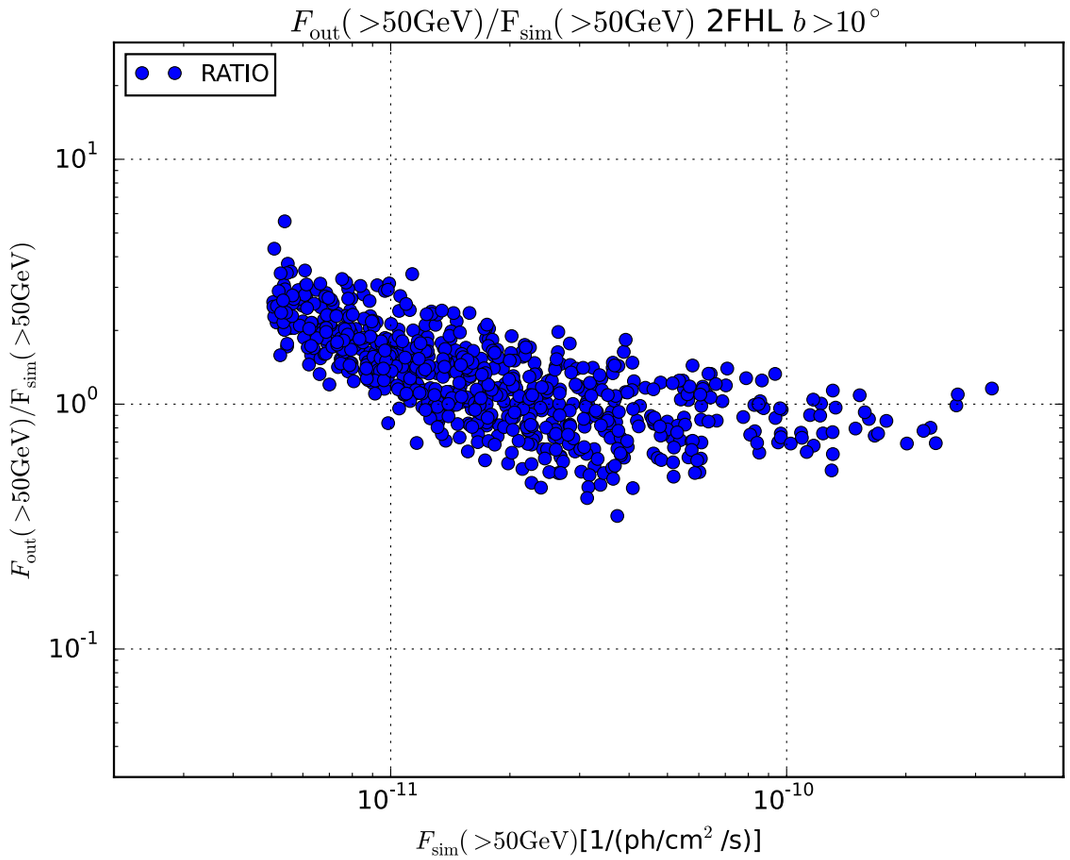

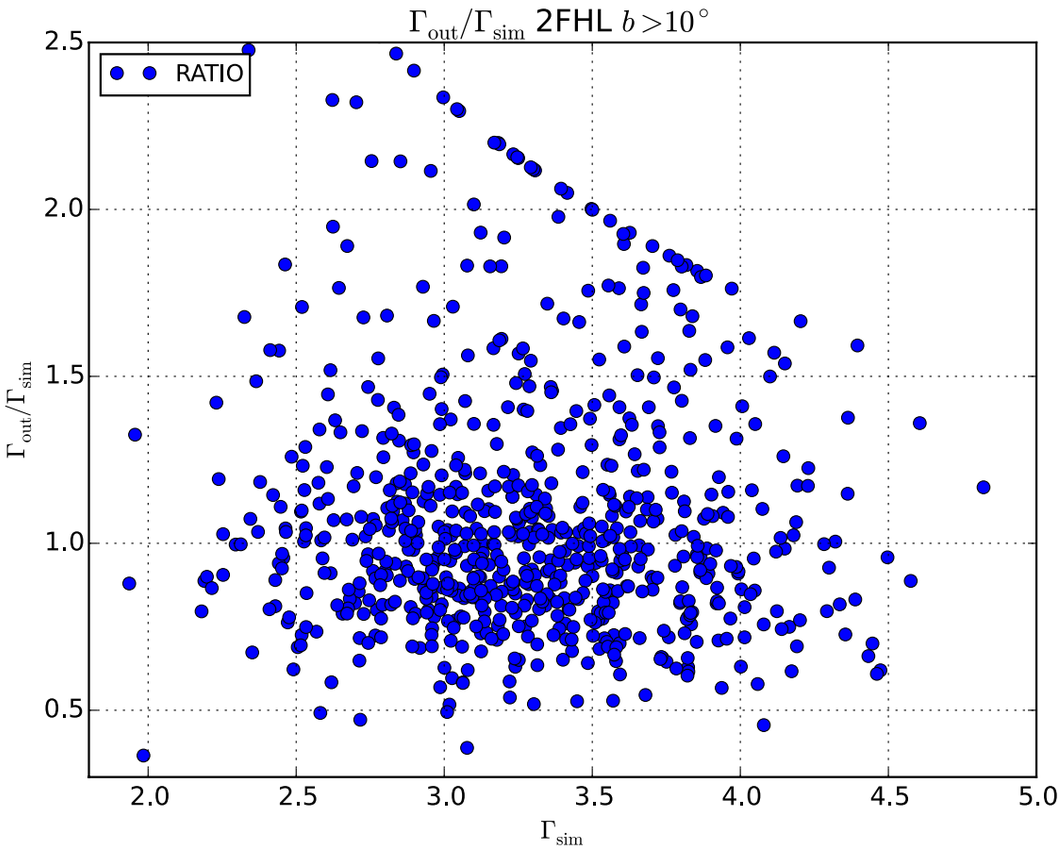

Γ Ratio

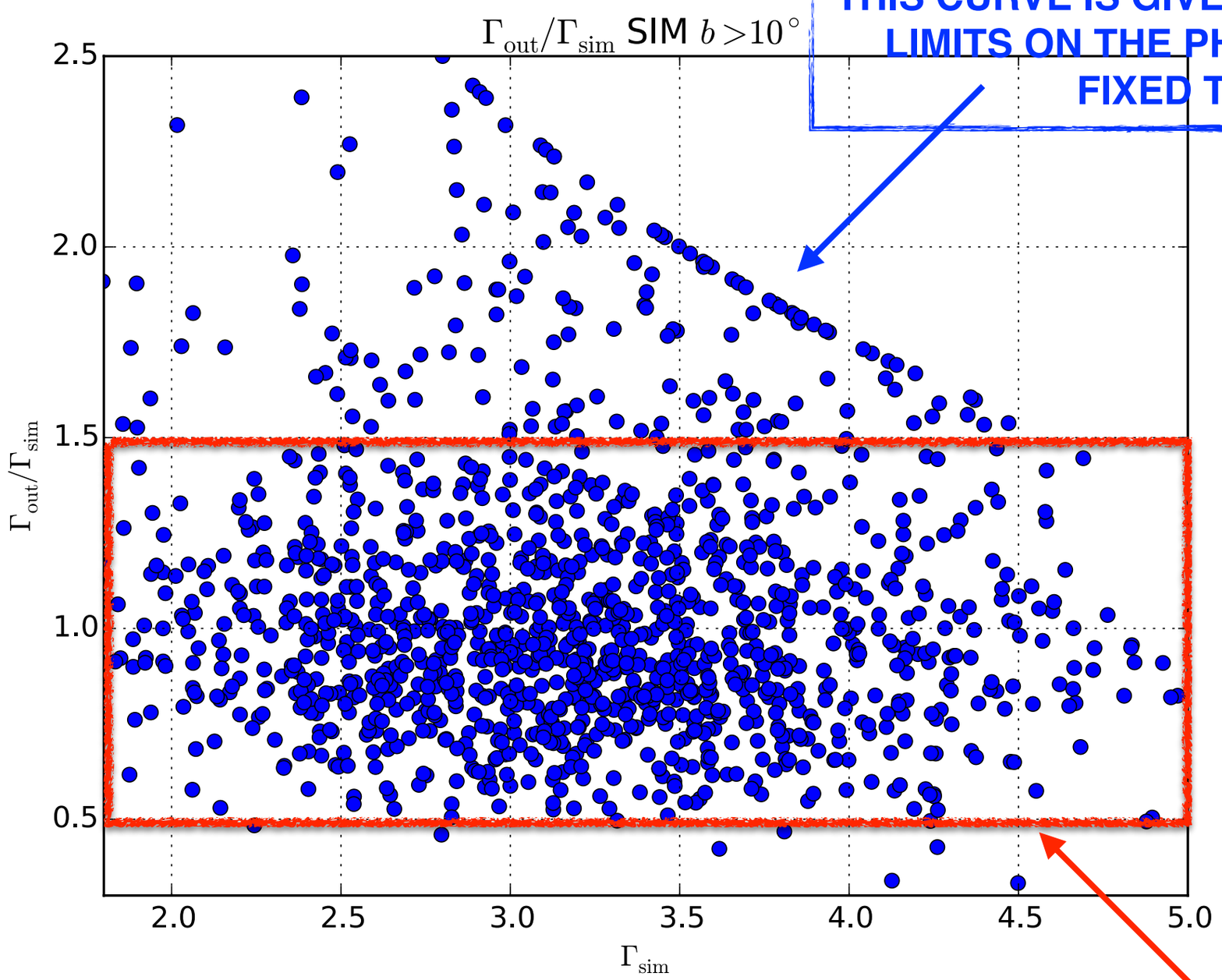

THIS CURVE IS GIVEN BY AN UPPER LIMITS ON THE PHOTON INDEX FIXED TO 7

THE MAJORITY OF SIMULATED SOURCES ARE HERE

dN/dΓ of the Simulation

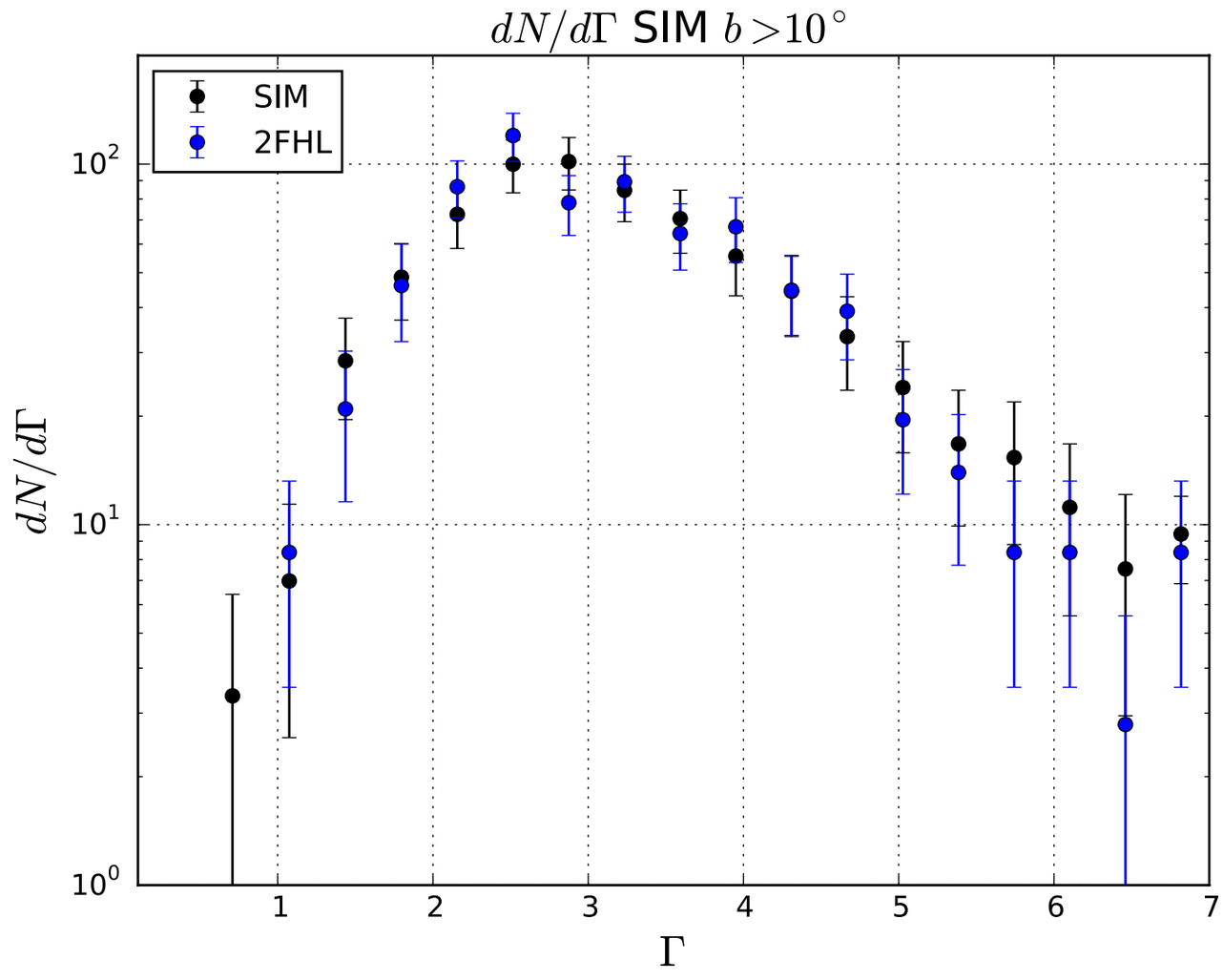

The photon index distribution of the analyzed simulations is consistent with the one of the 2FHL catalog

PIXEL COUNTING SENSITIVITY

- **In order to find the sensitivity of the pixel counting method we have considered a double broken power law with the first break at $1 \cdot 10^{-11}$ ph/cm^2/s and the second break ranging between $[0.5,5] \cdot 10^{-12}$ ph/cm^2/s.**
- **The slope above and below the first break is fixed to be 2.50 and 1.60 respectively.**
- **The slope below the second break is fixed to be 1.80 which is not the best fit value of the slope!**
- **We generate for each choice of the flux break 20 simulations and we compare the real sky and simulations pixel counting distributions with a χ^2 method.**

$S_{break(ph/cm2/s)}$	X^2
$5 \cdot 10^{-13}$	14
$7 \cdot 10^{-13}$	14
$1 \cdot 10^{-12}$	14
$1.3 \cdot 10^{-12}$	17
$1.5 \cdot 10^{-12}$	19
$2 \cdot 10^{-12}$	21
$3 \cdot 10^{-12}$	25
$5 \cdot 10^{-12}$	34

PIXEL COUNTING 2

- **We employed the photon fluctuation analysis to derive the shape of the flux distribution below the sensitivity if the 2FHL cat.**
- **Simulations with different value of the break and of the slope below the break have been tested.**
- **The flux distribution results to be consistent with a broken power law with a break in the range [0.8,1.5]$\cdot 10^{-11}$ ph/cm^2/s and a slope above and below the break α_1 = 2.50 and [1.6,1.75]**

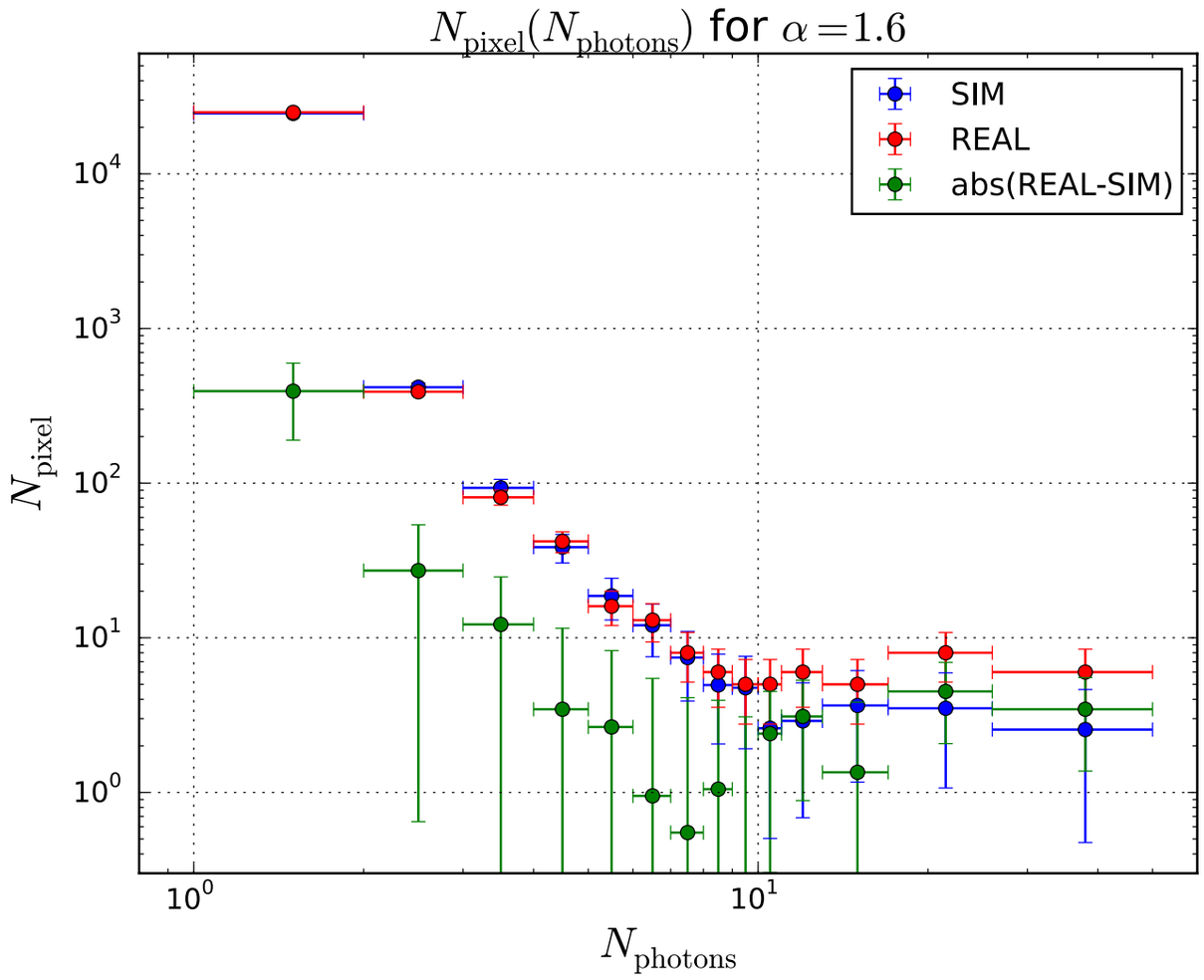

$S_{break(ph/cm2/s))}$	α_2	χ^2
$6 \cdot 10^{-12}$	1.40 ± 0.10	25.0
$8 \cdot 10^{-12}$	1.60 ± 0.03	15.5
$1 \cdot 10^{-11}$	1.60 ± 0.03	12.4
$1.5 \cdot 10^{-11}$	1.75 ± 0.03	14.6
$2 \cdot 10^{-11}$	1.85 ± 0.02	17.0

PIXEL COUNTING 3

- **The flux break can vary between [0.8,1,1.5]$\cdot 10^{-11}$ ph/cm^2/s with a slope below the threshold ranging between $\alpha_2 = [1.6,1.75]$.**
- **The choice of a break lower than 0.8$\cdot 10^{-11}$ ph/cm^2/s gives large value for χ^2.**
- **Our benchmark model for the flux differential distribution is a broken power-law with a break at 1$\cdot 10^{-11}$ ph/cm^2/s and with a slope above and below the break of $\alpha_1 = 2.50$ and $\alpha_2 = 1.60$ respectively.**

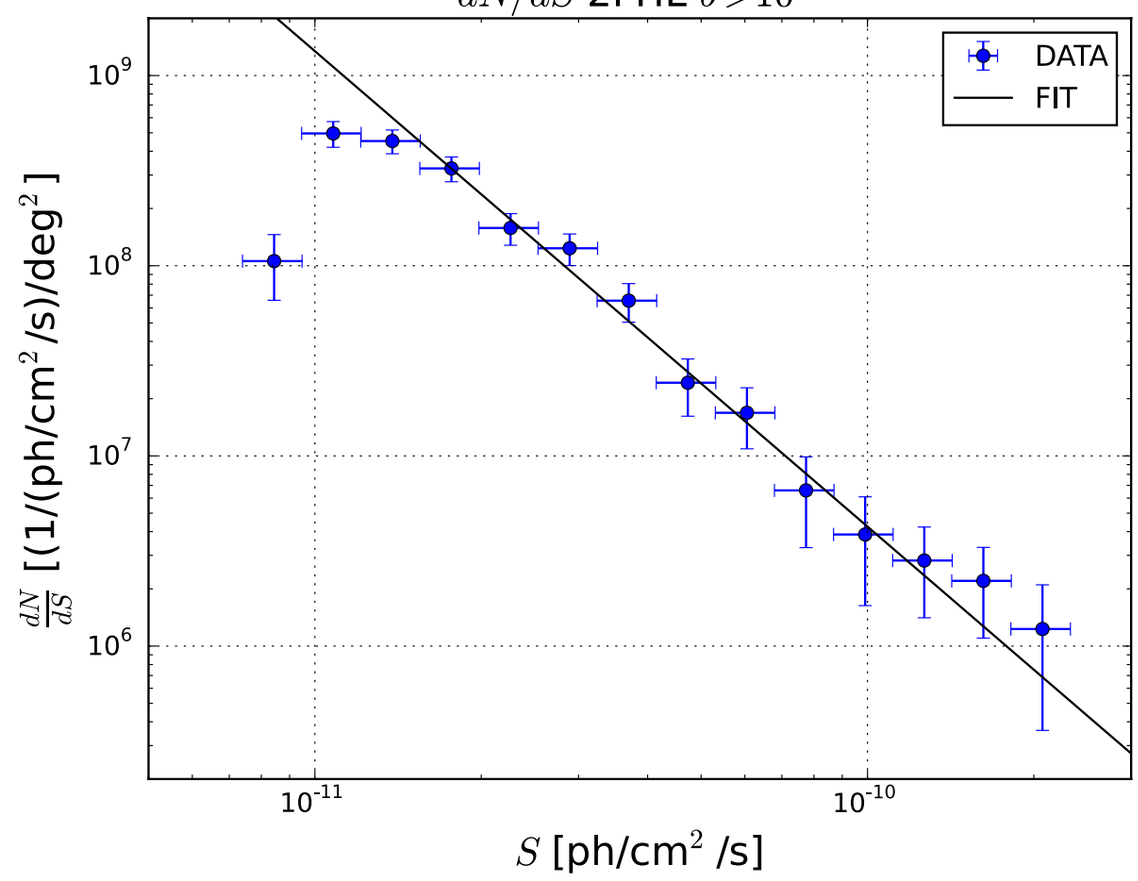

Evidence against star-forming galaxies as the dominant source of IceCube neutrinos

Keith Bechtol, M. Ahlers, M. Di Mauro, M Ajello and J. Vandenbroucke

arXiv:1511.00688 Submitted to PRL

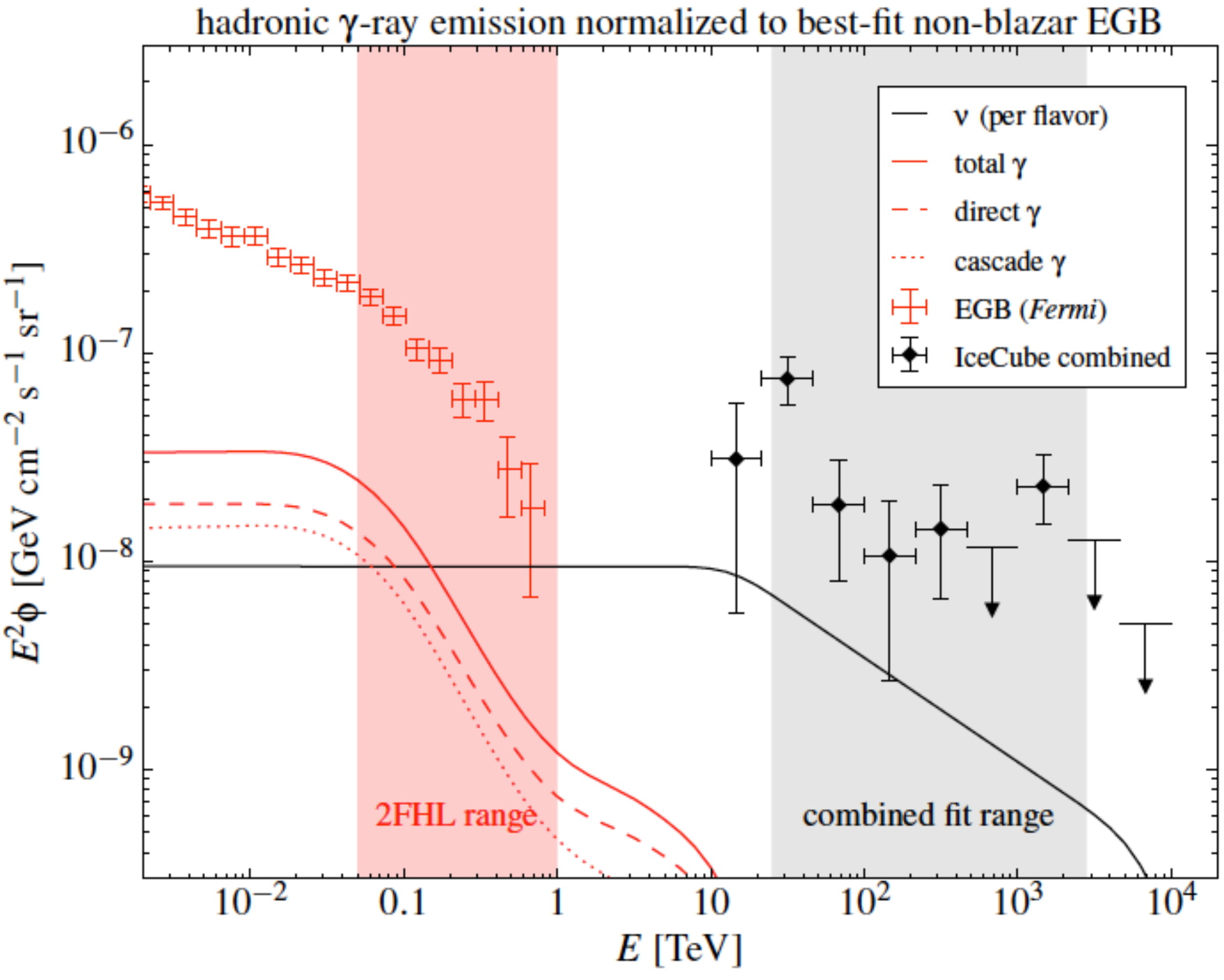

SPECTRAL ANALYSIS OF FERMI -LAT BLAZARS ABOVE 50 GEV

Alberto Dominguez and Marco Ajello

- **They present an analysis of the intrinsic (unattenuated by the extragalactic background light, EBL) power-law spectral indices of 128 extragalactic sources detected up to z=2.**
- **They find that our data are compatible with simulations that include intrinsic blazar curvature and EBL attenuation.**